

**ENTRAPPED GAS & EBULLITION IN PEAT:
TEMP & ATM PRESSURE**

EFFECTS OF TEMPERATURE AND ATMOSPHERIC PRESSURE
ON ENTRAPPED GAS AND EBULLITION IN PEAT

By

KRISTEN E. HARRISON B.E.S

A Thesis

Submitted to the School of Graduate Studies

In Partial Fulfillment of the Requirements

For the Degree

Master of Science

McMaster University

© Copyright by Kristen E. Harrison, January 2007

MASTER OF SCIENCE (2006)
(Geography)

McMaster University
Hamilton, Ontario

TITLE: Effects of atmospheric pressure and temperature on
entrapped gas and ebullition in peat

AUTHOR: Kristen E. Harrison

SUPERVISOR: Professor J. Michael Waddington

NUMBER OF PAGES: x, 88

ABSTRACT

Entrapped gas (V_g) greatly affects peatland biogeochemistry and hydrology by altering volumetric water content, buoyancy, hydraulic conductivity and generating over-pressure zones. These over pressure zones affect hydraulic gradients which influence water and nutrient flow direction and rate. The loss of this entrapped gas to the atmosphere via ebullition (bubbling) has been proposed as the dominant transport mechanisms for CH_4 from peatlands, releasing significant amounts of CH_4 to the atmosphere in a single event. Atmospheric pressure has been linked to ebullition events and is known to affect gas volumes; similarly, temperature affects gas production and volume. This thesis investigates the relationship between these environmental factors (atmospheric pressure and temperature) on both V_g and ebullition processes.

An incubation experiment using six peat cores at three incubation temperatures (4°C, 11°C, 20°C) was conducted in 2004 where each core was incubated in a sealed PVC cylinder and instrumented to measure V_g , pore-water CH_4 concentrations, and ebullition (volume and CH_4 concentrations). Temperature data for each incubation group and atmospheric pressure were measured within the laboratory setting.

Increasing bulk density was associated with decreased frequency of ebullition events and higher average ebullition volumes, indicating a relationship between bulk density ebullition characteristics. Future work will be needed to identify the direct relationship between V_g , bulk density and ebullition.

Evaluation of ebullition and atmospheric pressure data revealed a strong relationship between periods of falling pressure and ebullition events where 71% of measured events ($n = 391$) occurred during periods of decreasing pressure. Investigation of falling pressure characteristics revealed that drop duration (days) had a more significant effect on total ebullition volumes than did magnitude (kPa). As such, long periods of decreasing pressure trigger greater gas releases via ebullition than short decreases of large magnitude. This has implications for the prediction and modelling of ebullition events in natural systems, and for the estimation of CH_4 fluxes and carbon budgets of peatlands.

The V_g variability model accounted for changes in V_g caused by gas transfer between aqueous and gaseous phases (Henry's law) and thermal and pressure induced volume changes (Ideal gas law) using measured temperature and atmospheric pressure data. Gas loss via ebullition and CH_4 production were also accounted for. Good agreement was found between measured and modeled V_g values where gas contents were greater than 10% (average r^2 value of 0.78). Accuracy of the model indicates a general understanding of the processes, however it also suggests that further factors are influencing internal gas dynamics that require further investigation.

ACKNOWLEDGEMENTS

Funding for this research was provided by a NSERC Discovery grant awarded to Dr. J.M. Waddington. Thank you to Nirom Peat Moss Inc. for allowing access to the research site at St. Charles-de-Bellechasse, QC and of course to those who went out in the cold to collect the samples for this experiment.

Innumerable thanks go out to all those who have been involved in this research at its many stages: Marieke Oosterwoud and Dr. Erik Kellner who conducted the laboratory work and all those involved during those many weeks, to our undergraduate volunteers and interns, your hard work is always appreciated, PHAB research project members Dr. Erik Kellner and Dr. A.J. Baird for their continued inspiration, advice and expertise, and to Dr. J.E. Smith for research discussions and expertise. Many thanks must of course go to my committee members, Dr. Bourbonniere, Dr. Crowe, and Dr. Smith, your comments and suggestions have made this research stronger.

To my lab mates, Dr. Maria Strack, Jason Cagampan, Tim Duval, Dan Thompson and Maria Carol Lucchese, I send many thanks for bouncing ideas around with me, advice and insight; you have all been an important part of this research as well as being great friends and co-workers, we've had some good times. I would also like to send thanks out to Dr. J.S. Price for nudging me down the path of research.

Special thanks to my parents and family for their support, particularly to my husband Tim for helping me through each day with his constant support and understanding in my endeavours, wherever they take me.

For my supervisor, Dr. J.M. Waddington, I have great appreciation and respect. His efforts, dedication and support in my endeavours have been integral to this research, and will continue to be in future efforts. Dr. Waddington has endless energy for fuelling new and exciting research, and support for his students and peers. To him I say thank you, many times over.

TABLE OF CONTENTS

ABSTRACT	III
ACKNOWLEDGEMENTS	V
TABLE OF CONTENTS	VI
LIST OF FIGURES	VIII
LIST OF TABLES	IX
CHAPTER 1: INTRODUCTION.....	1
1.1 PEATLAND ECOSYSTEMS	1
<i>Peatlands and the carbon cycle</i>	<i>2</i>
1.2 EBULLITION AND ENTRAPPED GAS PROCESSES	4
<i>Entrapped biogenic gas</i>	<i>4</i>
<i>Ebullition.....</i>	<i>6</i>
<i>Implications for peatland hydrology.....</i>	<i>10</i>
<i>Implications for peatland biogeochemistry</i>	<i>14</i>
<i>Implications for carbon budgets</i>	<i>15</i>
1.3 OBJECTIVES	16
CHAPTER 2: METHODS	19
2.1 EXPERIMENTAL DESIGN.....	19
2.2 STUDY AREA	20
2.3 LABORATORY EXPERIMENT	20
<i>Peat cylinder preparation and design.....</i>	<i>20</i>
<i>CH₄ ebullition and pore-water.....</i>	<i>22</i>
<i>Entrapped gas content</i>	<i>22</i>
<i>Atmospheric pressure and temperature</i>	<i>23</i>
<i>Bulk density.....</i>	<i>24</i>
2.4 V _G VARIABILITY	24
<i>CH₄ equilibrium aqueous phase concentrations.....</i>	<i>24</i>
<i>V_g variability model</i>	<i>26</i>
2.5 ATMOSPHERIC PRESSURE AND EBULLITION RELATIONSHIP	27
CHAPTER 3: ENTRAPPED GAS AND POREWATER: RESULTS AND DISCUSSION	29
3.1 RESULTS.....	29
<i>Peat characteristics</i>	<i>29</i>
<i>Pore-water CH₄ concentrations.....</i>	<i>31</i>
<i>Entrapped gas content</i>	<i>36</i>
3.2 DISCUSSION.....	43
<i>Effect of capping cylinders.....</i>	<i>43</i>
<i>Gas phase establishment.....</i>	<i>44</i>
<i>Gas distribution and bulk density</i>	<i>47</i>

<i>Pore-water and gas content</i>	48
<i>Implications</i>	50
CHAPTER 4: BIOGENIC GAS EBULLITION.....	52
4.1 RESULTS.....	52
<i>Ebullition</i>	56
<i>Statistical Analysis</i>	60
4.2 DISCUSSION.....	63
<i>Entrapped gas variability</i>	63
<i>Ebullition variability</i>	65
<i>The ebullition-pressure relationship</i>	68
<i>Implications</i>	70
CHAPTER 5: MODELING ENTRAPPED GAS CONTENT.....	73
5.1 RESULTS.....	73
<i>Modeled entrapped gas content</i>	73
5.2 DISCUSSION.....	78
<i>Modeled entrapped gas content</i>	78
CHAPTER 6: CONCLUSIONS	80
REFERENCES.....	84

LIST OF FIGURES

Figure 1.1: As bubbles accumulate (A) they block pores, and can effectively block off entire zones (B). As bubbles continue to accumulate within these zones, they can become over-pressurized (C) (Kellner <i>et al.</i> , 2005).....	11
Figure 2.1: Cylinder equipment set-up: A) Illustrative diagram, B) working cylinder set-up. See text for details.....	21
Figure 3.1: Cylinder bulk densities with depth from the peat surface and one standard deviation error bars.....	30
Figure 3.2: CH ₄ pore-water concentrations for the upper (U) and Lower (L) portions of each cylinder in mg CH ₄ l ⁻¹	32
Figure 3.3: CH ₄ concentrations (%CH ₄) in ebullition gas (shown as percent CH ₄) by volume.....	36
Figure 3.4: TDR-measured entrapped gas content for all cylinders. C3, C4 and C5 are shown across the change in incubation temperature from 11°C (up to day 78) and 20°C for the remainder of the experiment.....	39
Figure 3.5: Cumulative change in entrapped gas (ΔV_g) generated from TDR-measured gas contents for Upper (grey) and Lower (black) portions of each cylinder.....	42
Figure 4.1: TDR-measured entrapped gas contents for Upper (grey) and Lower (black) portions of each cylinder. Note the patterns of increasing V_g in all cylinders. C3, C4, C5 are incubated at 11°C until day 78 and at 20°C from day 79-172.....	55
Figure 4.2: Extracted ebullition volumes (ml) for cylinders 1, 3, 4 and 5. C6 showed no signs of active ebullition.....	57
Figure 4.3: Extracted ebullition volume for C1 and atmospheric pressure.....	59
Figure 5.1: Measured and calculated ΔV_g values for C1 and C3. The black line indicates measured ΔV_g , calculated ΔV_g values for the P, T, Prod. & Eb and the P & T models are indicated by the dark grey and light grey lines respectively.....	76
Figure 5.2: Scatter plots of measured ΔV_g values against calculated values for the model that best fits the measured data. Measured C1U values are plotted against the P&T model, the remainder of the cylinder locations are plotted against calculated values from the P, T, Prod. & Eb model.....	77

LIST OF TABLES

Table 3.1: Bulk density (g cm^{-3}) averages for upper and lower portions of each cylinder.....	30
Table 3.2: Pore-water CH_4 concentration values for each cylinder at both the upper and lower probe locations.....	33
Table 3.3: Theoretical CH_4 equilibrium aqueous phase concentrations (EAPC) (mg l^{-1}) for two bubble diameters (0.00001 cm and 0.01 cm) for each incubation temperature (20°C, 11°C, and 4°C) and for each scenario (100% CH_4 and 20% CH_4 where the balance is N_2 and water vapour) are shown.....	34
Table 3.4: Initial gas contents following wetting at experiment onset by cylinder and probe location.....	37
Table 3.5: Average rates of accumulation in V_g for the period prior to climate chamber failure (day 78) and following failure (day 79) to the end of the experiment. Calculated as the slope of the line between average gas contents, these values represent an average rate of accumulation for these cylinders.....	37
Table 3.6: Cylinder change in entrapped gas content (ΔV_g) by incubation temperature and probe location.....	41
Table 4.1: ΔV_g ranges, and variability for all cylinders. Range over which V_g for each cylinder occurs, compared with entrapped gas variability maximums, and range. C3, C4 and C5 at 11°C are for days 4-78 (excludes initial drop in V_g due to dissolution of entrapped air after wetting), and days 79-172 for the 20°C temperature group.....	54
Table 4.2: Experiment total and cylinder average Volume (ml) and Flux ($\text{mg m}^{-2} \text{d}^{-1}$) data for ebullition events from cylinders 1, 3, 4, and 5.....	58
Table 4.3: Ebullition events by cylinder and percent occurrence based on direction of atmospheric pressure change, where % +P Ebullition and % -P Ebullition represent the percent of ebullition occurrences during periods of increasing and decreasing pressure respectively.....	60
Table 4.4: P-values for linear regressions between Total Ebullition Volume (dependent variable) and the independent pressure characteristics (Magnitude, Duration and Rate) and combined variable groups, MD (Magnitude & Duration), MR (Magnitude & Rate) DR (Duration and Rate) and MDR (Magnitude, Duration & Rate). Relationships with a 90% confidence interval ($P < 0.100$) are significant and shown shaded.....	61

Table 4.5: P-values showing the relative significance of each independent variable (Magnitude, Duration and Rate) in a combination for predicting Total Volume as a dependent variable. This provides insight into the effect of each relative to one another for predicting Total Volume.....62

Table 5.1: Production values (ml d^{-1}) used in the model. CH_4 production values ($\text{ug g}^{-1} \text{d}^{-1}$) were based on average ebullition CH_4 concentration per cylinder. The number of days over which each production value was applied are also presented. Values are in order of use from the beginning to the end of the model dataset (days 210-330, 120 days).....73

Table 5.2: r^2 values based on measured ΔV_g values and ΔV_g as calculated by the model accounting for atmospheric pressure and temperature changes only (P&T) and where pressure, temperature, production and ebullition were included (P, T, Prod & Eb.).....74

CHAPTER 1: INTRODUCTION

1.1 Peatland ecosystems

Peatlands are most commonly found in the boreal and sub-arctic regions of the World, although they are not exclusive to these regions (Gorham, 1991). Peatlands occupy an area of $\sim 346 \times 10^6$ ha worldwide, of which about 119×10^6 ha are in Canada (Gorham, 1991). Natural peatland ecosystems are characterized by the accumulation of organic deposits (peat) composed of a variety of peat-forming vegetation, including sedges, rushes, and brown and *Sphagnum* mosses to a depth of >30-40 cm. Peat accumulates when the rate of production is greater than that of decomposition (Clymo, 1983). *Sphagnum* dominated peatlands are the most prominent of the peat-forming communities and can be commonly found in bogs and fens. Bogs are generally disconnected from local groundwater systems receiving all water and nutrient inputs from atmospheric sources, creating ombrotrophic (nutrient poor) conditions (Clymo, 1983). These conditions are conducive to *Sphagnum* growth, and covered with varying degrees of sedge, shrub and tree cover. Fens are fed by slow-moving groundwater inputs with nutrient supply dependent on the flow rate and nutrient availability within the water source. Considered minerotrophic, fens can be either oligotrophic (nutrient poor) or eutrophic (nutrient rich), with oligotrophic fens being more *Sphagnum* dominated with varying degrees of sedge, shrub and tree cover, and with increasing sedge, and brown moss dominance as nutrient levels increase (Mitsch and Gosselink, 2000).

Sphagnum peat profiles are often diplotelmic, consisting of an upper active layer (acrotelm) where new *Sphagnum* growth and photosynthesis occur, underlain by a thicker

catotelm composed of the partially decomposed plant materials from the growth of previous years (Ingram, 1992). The acrotelm is composed of loose, poorly decomposed organic material with a high porosity (>90%) and large pore structures, low bulk density and high hydraulic conductivity (Boelter, 1965). These characteristics generate a high specific yield and water storativity, maintaining a shallow water table with minimal fluctuations (Price, 1996; Ingram, 1983). In comparison, the catotelm, located below the water table, is composed of more compressed and decomposed organic materials resulting in smaller pores, although retaining a high porosity. As a result of further decomposition and compression, the catotelm has higher bulk densities, and hydraulic conductivities that decrease with depth through the profile (Boelter, 1965). Hydraulic conductivities in catotelmic peat are very low, generally in the order of 10^{-5} m s^{-1} , and assumed temporally constant (Boelter, 1965).

Peatlands and the carbon cycle

As each season adds new plant debris, growth from previous years moves further down the peat profile, in time entering the anaerobic zone, where decomposition slows significantly, allowing materials to accumulate over centuries or millennia generating peat deposits of several meters (Gorham, 1991). This process of storing organic material acts as a net carbon sink, sequestering between $23\text{-}29 \text{ g C m}^{-2} \text{ yr}^{-1}$ (Gorham, 1991). This equates to $\sim 450 \text{ Gt C}$ or approximately one third of the terrestrial carbon stores being held in peatlands (Gorham, 1991).

In addition to CO₂, decomposition of organic materials produces other biogenic gases including CH₄ and H₂S (Strack *et al.*, 2005; Kellner *et al.*, 2005). While natural peatlands act as sinks for atmospheric CO₂, they are a net source of CH₄ to the atmosphere, releasing ~4 g C m⁻² yr⁻¹ (Gorham, 1991). Methane emission rates depend on the balance between methane production (methanogenesis), and oxidation (Knowles, 1993; Walter *et al.*, 1996; Segers, 1998), the conditions for which vary across the hummock-lawn-hollow microtopography commonly found in natural peatlands (Knowles, 1993; Waddington and Roulet, 1996). Methanogenesis occurs under reduced, anaerobic conditions found below the water table in peatlands, whereas oxidation requires aerobic conditions (Knowles, 1993; Segers, 1998) such that hollows, which have little or no aerobic zone, have higher rates of CH₄ flux than hummocks which have thicker aerobic zones (Waddington and Roulet, 1996; Strack *et al.*, 2005). Waddington and Roulet (1996) found both hummocks and hollows to be annual sources of CH₄ with fluxes of 8.1 to 9.8 g m² yr⁻¹ from hollows and 0.0 and 0.2 g m² yr⁻¹ from hummocks.

CH₄ is transported to the atmosphere via diffusion, plant transport, and ebullition (bubbling) (Fechner-Levy and Hemond, 1996), with several studies suggesting that ebullition is the dominant transport mechanism from natural peatlands (Fechner-Levy and Hemond, 1996). Traditional chamber methods used to estimate CH₄ fluxes from peatlands can account for diffusive and plant transported CH₄ fluxes, however, they do not effectively account for ebullition events. This is because ebullition events are both temporally and spatially variable (e.g. Romanowicz *et al.*, 1995; Glaser *et al.*, 2004; Baird *et al.*, 2004), making them difficult to capture and study. The processes involved in the

development and subsequent release of gas via ebullition are not well understood, and are the focus of this study.

1.2 Ebullition and entrapped gas processes

Entrapped biogenic gas

Although it is commonly assumed, full saturation is not a requisite condition of soils below the water table (Baird and Waldron, 2003). In mineral soils, the presence of bubbles is often attributed to air entrapment during water table rise, or infiltration (e.g., Constantz *et al.*, 1988; Fayer and Hillel, 1986); however, this process is not implicated as the main source of entrapped gas in peat. Although some air entrapment may occur in shallow peat depths, gas bubbles also occur deep within peat columns (e.g. Romanowicz *et al.*, 1995; Fechner-Levy and Hemond, 1996), suggesting additional sources and mechanisms for their existence.

Numerous studies (e.g., Ivanov, 1981; Brown *et al.*, 1989; Buttler *et al.*, 1991; Romanowicz *et al.*, 1995; Baird and Waldron, 2003) have suggested that in situ production of biogenic gases during decomposition as the mechanism responsible for the generation of a gas phase in peat. As gases (CO₂, CH₄ and H₂S) are produced during the decomposition of organic materials they accumulate dissolved in peat pore-water (Whalen and Reeburgh, 1990). Two possible mechanisms are involved in the transfer of these gases from the aqueous phase to the gaseous phase in peat. Classical bubble formation theory in lakes requires that concentrations in the aqueous phase surpass their relative solubility threshold (equilibrium concentration) allowing them to come out of

solution forming bubbles (Hutchinson, 1957). This method of bubble formation is currently used in several physically based wetland CH₄ models that account for ebullition processes, and require pore-water concentrations to exceed 7.1-8.0 mg CH₄ l⁻¹ (e.g., Walter *et al.*, 1996; Granberg *et al.*, 2001). Recent work has shown that although gases can accumulate beyond this threshold (Dinel *et al.*, 1988; Brown *et al.*, 1989) bubble generation also occurs at much lower concentrations (0.1-1.5 mg CH₄ l⁻¹) (Baird *et al.*, 2004). Baird *et al.* (2004) suggest two possible causes for this: 1) in near surface peat, air bubbles that become entrapped during water table fluctuations can act as points of focus for further bubble growth; and 2) high degrees of variability in pore-water concentration on small spatial scales may not be properly represented by measurement techniques, thus allowing for high concentrations in areas not sampled to generate bubbles according to classical bubble formation theory. Regardless, once a gas phase has been initiated within the peat, the further production of biogenic gases will continue to increase entrapped gas volumes within the peat pore structure.

Evidence for the presence of entrapped gas has been shown in both field (e.g. Romanowicz *et al.*, 1995; Fechner-Levy and Hemond, 1996; Glaser *et al.*, 2004; Comas *et al.*, 2005; Tokida *et al.*, 2005a; Strack *et al.*, 2005) and laboratory (e.g. Reynolds *et al.*, 1992; Beckwith and Baird, 2001; Baird and Waldron, 2003; Tokida *et al.*, 2005b) studies. For example, using cores of re-packed peat Reynolds *et al.* (1992) measured gas contents of up to 30%, higher than contents reported by other authors using intact peat cores who measured contents of 5-12% (Beckwith and Baird, 2001; Baird and Waldron, 2003). Rosenberry *et al.* (2003) measured gas contents of 9-13% from a raised bog field site in

the Glacial Lake Agassiz region of Minnesota. Comas *et al.* (2005) employed two ground-penetrating radar (GPR) techniques to measure in situ entrapped gas content spatially and with depth through a peatland at the Caribou Bog in Maine, finding entrapped gas contents ranging from 0-10%. Similar gas contents were also reported by Kellner *et al.* (2005), and Tokida *et al.* (2005a) with gas content ranges of 4-15% and 0-19%, respectively.

Layers of dense peat, such as root mats, may act as confining layers for entrapped bubbles, preventing movement to the surface. At a single location, succession of vegetation can cause repeated changes in microform between hummocks, lawns and hollows, with accompanying changes in vegetation (*Sphagnum*, sedges, shrubs and trees) (Belyea and Clymo, 2001). Hollows are generally composed of loosely packed *Sphagnum*, resulting in low bulk densities when compared with hummock forming vegetation species which may develop a thick root mat, containing woody debris. With each year's new growth, previous vegetation is incorporated into the peat structure generating highly variable patterns in bulk density, varying on the order of tens of centimetres (Belyea and Clymo, 2001).

Ebullition

Ebullition occurs when the buoyant forces of entrapped gas exceed the forces restraining it (Fechner-Levy and Hemond, 1996; Strack *et al.*, 2005) allowing the gas to escape to the atmosphere as bubbles. Evidence of this has been found in both laboratory (Baird *et al.*, 2004; Kellner *et al.*, 2006) and field (Strack *et al.*, 2005) experiments. Baird

et al. (2004) suggested that peat structure might be a significant factor in the development of the gas threshold for peat, however to date no work has been published directly investigating this. Baird *et al.* (2004) found a threshold limit of approximately 10-14% while Kellner *et al.* (2006) found that similar gas content threshold values of 12 and 15% provided very good results when modelling ebullition events.

In order for ebullition to occur, the entrapped gas volume must exceed the threshold gas level. Alone, bacterial production of gas could accumulate a volume sufficient to exceed the threshold limit and initiate an ebullition event (Glaser *et al.*, 2004) to then begin accumulation again. Entrapped gas volumes, however, are also affected by changes in pressure and temperature according to Henry's law (HL) and the Ideal gas law (IGL) (Kellner *et al.*, 2005). Changes in both temperature and pressure elicit responses in solubility (HL) and gas volume caused by thermal and pressure-induced expansion and contraction of gas (IGL). So that as temperatures increase moving into the summer months there would not only be an increase in bacterial gas production, but also an increase in volume caused by the transfer of poorly soluble gases (particularly CH₄) out of solution, and the thermal expansion of the existing entrapped gas (Strack *et al.*, 2005). Strack *et al.* (2005) found evidence of this seasonal fluctuation with increases in gas content of 7 and 15% over two summer seasons at the same field site.

Smaller, more frequent changes in gas volume due to changes in weather patterns can also generate fluctuations in entrapped gas volumes (Fechner-Levy and Hemond, 1996; Glaser *et al.*, 2004). For example, reduced solubility and expansion of gas during

periods of low pressure often occur with warmer air masses. The link between periods of low atmospheric pressure and ebullition has since been confirmed in both field (Fechner-Levy and Hemond, 1996; Glaser *et al.*, 2004; Strack *et al.*, 2005) and laboratory (e.g. Tokida *et al.*, 2005; Kellner *et al.*, 2006) experiments.

Despite having identified these relationships, ebullition events are still relatively poorly understood. Due to their high variability, ebullition events are not easily measured in the field. Field evidence of ebullition has been shown using proxy measurements such as significant changes in dissolved CH₄ concentrations (Romanowicz *et al.*, 1995), changes in surface elevation (Fechner-Levy and Hemond, 1996; Glaser *et al.*, 2004), and more recently using gas traps to directly measure ebullition at fixed locations (Strack *et al.*, 2005). Recent laboratory investigations (Baird *et al.*, 2004; Tokida *et al.*, 2005b; Kellner *et al.*, 2006) have provided insight into ebullition processes as well. Using an assumed initial entrapped gas content, and by combining Henry's law and the Ideal gas law, differentiating with respect to pressure, Tokida *et al.* (2005b) calculated changes in gas volume caused by changes in atmospheric pressure according to:

$$\frac{\partial V_g}{\partial P} = -\frac{V_g}{P} - \frac{V_w RT}{PH_d} \quad [1]$$

where V_g is the volume of gas (m³), V_w is the volume of water containing V_g (m³), P is the pressure (Pa) (where gas pressure is assumed equal inside and outside so that pressure is atmospheric pressure + pore-water pressure), R is the universal ideal gas constant (J mol⁻¹

K^{-1}), T is the temperature (K), and H_d is the constant of Henry's law ($J\ mol^{-1}$) (as presented in Kellner *et al.*, 2006).

Good agreement was found between the calculated changes due to pressure decreases, and the volumes from ebullition flux data (Tokida *et al.*, 2005b), further confirming the relationship between atmospheric pressure and ebullition.

More recently, Kellner *et al.* (2006) combined the equation from Tokida *et al.*, (2005b) [1] and an equation to account for volume change generated by temperature fluctuations by combining HL and IGL and differentiating with respect to temperature (Fechner-Levy and Hemond 1996, as presented in Kellner *et al.*, 2006):

$$\frac{\partial V_g}{\partial T} = \frac{V_g}{T} + \frac{V_w RT}{H_d^2} \times \frac{\partial H_d}{\partial T} \quad [2]$$

Iterations for each gas species present provided changes in total entrapped gas volume, so that when combined with a production term, and a gas threshold, Kellner *et al.* (2006) were able to model ebullition events measured during a laboratory experiment.

Frequency of ebullition events is therefore likely a function of peat threshold, gas production and environmental factors that affect gas volume. Results from two laboratory experiments investigating ebullition reported average ebullition volumes of $32.4\ ml\ d^{-1}$ at an incubation temperature of $\sim 20^\circ C$ (Kellner *et al.* 2006) and a lower average value of $4.7\ ml\ d^{-1}$ at $\sim 12^\circ C$ was found by Baird *et al.* (2004). This shows that under realistic incubation temperatures ebullition processes are able to transfer significant amounts of gas to the atmosphere. CH_4 concentrations for individual ebullition events are

highly variable, but average concentrations are generally quite high with values of 57% and ~60% CH₄ by volume reported by Kellner *et al.* (2006) and Tokida *et al.* (2005b) respectively.

Implications for peatland hydrology

As bubbles form, it is probable that they develop attached to peat fibres or within the voids between fibres (Kellner *et al.*, 2005). Bubbles of smaller diameter than the surrounding pore throats have the ability to move freely when induced until they encounter some restriction such as increased bubble size (aggregation, volume change or production), smaller pores or other bubbles that have been trapped. When a pore diameter is smaller than that of the bubble, the bubble becomes trapped, blocking off the pore opening (Kellner *et al.*, 2005). As more bubbles block off voids, they have the potential to greatly reduce water and solute transfer from surrounding areas (Kellner *et al.*, 2005). As bubbles continue to develop inside these closed regions, they can create zones of elevated pore-water pressure (Figure 1.1 a,b,c). Evidence of this process in the form of flow-reversals (Devito *et al.*, 1997; Glaser *et al.*, 2004) and forcible ejection of water during piezometer installation (Romanowicz *et al.*, 1995) has been found in field studies and has been measured directly using pressure transducers (Glaser *et al.*, 2004; Kellner *et al.*, 2005).

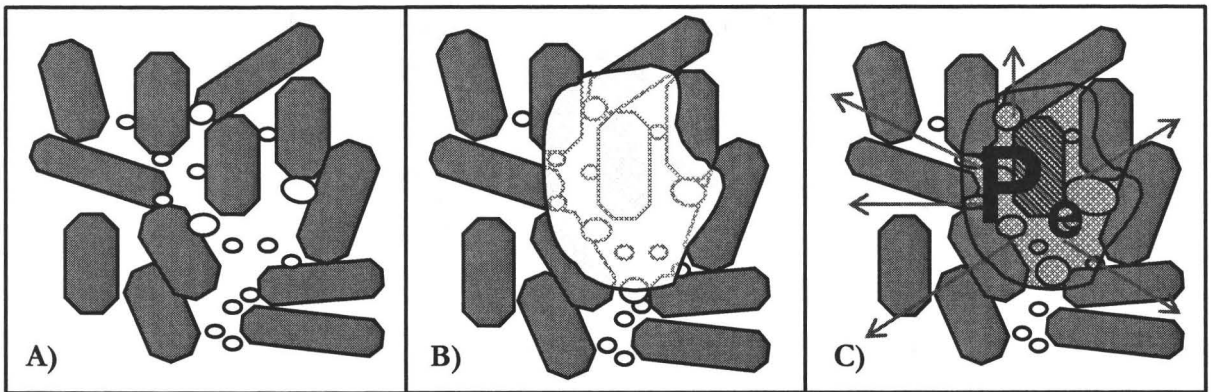


Figure 1.1: As bubbles accumulate (A) they block pores, and can effectively block off entire zones (B). As bubbles continue to accumulate within these zones, they can become over-pressurized (C) (Kellner *et al.*, 2005).

As bubbles become entrapped, they reduce effective porosity, decreasing hydraulic conductivity in biogenically active peats (Baird *et al.*, 2001; Kellner *et al.*, 2005). This effect was likely first suggested by Waine *et al.* (1985), although not explicitly studied in this work. Later work (e.g. Reynolds *et al.* 1992; Faybishenko, 1995) used re-packed peat columns, high incubation temperatures and large hydraulic gradients to study the effects of entrapped gas on hydraulic conductivity. Beckwith and Baird (2001) and Baird and Waldron (2003) expanded upon this work using intact peat samples under more realistic incubation temperatures and hydraulic gradients. As gas develops within peat, the degree of saturation decreases, assumedly caused by the displacement of water by biogenic gas as it accumulates (Beckwith and Baird, 2001). In laboratory studies, entrapped gas volumes appear to increase from initiation of the experiment, reaching a maximum value around which they fluctuate (Baird *et al.*, 2004; Kellner *et al.*, 2006) an indication of the threshold proposed by Baird *et al.* (2004). As the entrapped gas content increases, the hydraulic conductivity of peat decreases, such

that Baird and Waldron (2003) found an increase in gas content of only 1-2% generated an order of magnitude decrease in hydraulic conductivity. This then has large implications for variability of hydraulic conductivity in natural peatlands seasonally, and potentially on a much more frequent basis in the order of days or hours as entrapped gas volumes change in response to environmental conditions and ebullition (Strack *et al.*, 2005). At the seasonal scale and with changes in environmental conditions, gas variation would be marked across a peatland, and could possibly be evident regionally in biogenically active peat. The effect of ebullition on hydraulic conductivity would have a localized effect seen on the scale of centimetres or meters depending on the size and depth of the entrapped gas volume released (Kellner *et al.*, 2005).

The processes of entrapped gas that affect hydraulic conductivity also have effects on water storage, water table position, buoyancy and peat volume. Due to the displacement of water for a given increase in gas content, there is an equal and opposite change in water content (Kellner *et al.*, 2005). This displacement not only lowers water content, but also by its function decreases the specific yield and raises the water table. This then can affect the apparent water budget for a peatland as these conditions change temporally and spatially throughout the season. For example, a decrease in atmospheric pressure could instigate a rise in water table, and decreases in water content and specific yield. The effects of water displacement on water table height are balanced by changes in buoyancy and peat volume generated by entrapped gas fluctuation. Peat is a highly compressible media (Price, 2003), allowing for volume changes to occur in response to variations in total stress acting upon it. The low density of gases compared to that of

water, increase the buoyant forces acting upon the peat matrix, reducing effective stress and therefore decreasing compression of the peat matrix with depth where entrapped gas exists (Kellner *et al.*, 2004; Strack *et al.*, 2005). This effect is particularly important in low-density peat such as quaking (floating) mats or hollows where the peat is composed of loosely packed materials and are essentially ‘floating’ (Strack *et al.*, 2005). These low-density, high porosity peats are more acutely affected by compression changes due to the high potential for deformation (Price, 2003; Strack *et al.*, 2005). Zones of elevated pore-water pressure also cause peat expansion, due to the excess pressure exerting outward pressure from within these closed zones, adding to the effects of other peat expansion (see Kellner *et al.*, 2005). As peat density increases with depth, these effects become less evident and larger volumes of gas are required to elicit significant responses (e.g. Glaser *et al.*, 2004). The effect of peat volume change on surface elevation will affect water table position in the opposite direction as the forces of water displacement. For example, an increase in gas will displace water shifting the water table up, but will also increase buoyancy causing peat expansion, shifting the water table lower with the result being that the opposing influences of these processes together act to minimize water table fluctuations in peatlands (Kellner *et al.*, 2005). Ebullition and the abrupt movement of gas within the peat profile can cause sudden increases or decreases in gas content at a particular location. The effects of these gas movements are generally small in scale, affecting only localized areas in shallow peat zones (Kellner *et al.*, 2005), but have been noted on a large scale in deep peat (Romanowicz *et al.*, 1995; Fechner-Levy and Hemond, 1996; Rosenberry *et al.*, 2003).

Implications for peatland biogeochemistry

Peatland hydrology is highly coupled with peatland ecology, chemistry and other functions, where a change in one brings about changes in the other. Entrapped gas in peat is an example of this. Zones of elevated pore-water pressure generate flow reversals, as indicated by changes in hydraulic gradients (e.g. Waddington and Roulet, 1997). These flow reversals then affect nutrient and contaminant transport pathways, in turn changing the availability of labile carbon and other substrates for CH₄ production, vegetation growth, etc. (Strack *et al.*, 2005). In a field study by Waddington and Roulet (1997) hydraulic gradients changed over the summer season from an initial downward flow (recharge) to outward radial flow following a period of drought; transporting water, nutrients, minerals and carbon towards the outer margins and surface of the peatland (Waddington and Roulet, 1997).

On a smaller scale, entrapped gas bubbles can affect the flow of solutes by generating large concentration gradients (Strack *et al.*, 2005). The potential for very high concentrations of gas, particularly CH₄, can generate large concentration gradients between bubbles and surrounding pore-waters, influencing diffusive fluxes depending on bubble concentration (Strack *et al.*, 2005). By accounting for the influence of bubbles on concentration gradients, Rothfuss and Conrad (1998) were able to better estimate diffusive fluxes from rice paddy soil that could be analogous to processes in peat.

Changes in buoyancy induced by entrapped gas volumes plays a significant role in ecosystem structure and function, particularly for floating peat mats (Strack *et al.*, 2005).

Entrapped gas in floating peat mats allow these systems to fluctuate with water levels, up to a potential ratio of 1:1 where there is no connection to a rigid peat column (Roulet, 1991; Strack *et al.*, 2005). By being able to fluctuate with the water table, these systems can maintain water table levels, and oligotrophic conditions conducive to *Sphagnum* growth (Mallik, 1989; Strack *et al.*, 2005).

Implications for carbon budgets

Ebullition processes significantly increase estimates of CH₄ release to the atmosphere, with potentially major impacts to current carbon balance calculations and the proportion contributed by northern peatlands to the global carbon cycle (Tokida *et al.*, 2005b).

As previously discussed, CH₄ concentrations in ebullition gas volumes are relatively variable. Average values of ~60% CH₄ by volume (Tokida *et al.*, 2005; Kellner *et al.*, 2006) generate significant fluxes to the atmosphere when applied to average ebullition event volumes found by Kellner *et al.* (2006) releasing 98.5 g CH₄ m⁻² yr⁻¹ to the atmosphere, approximately 24 times the average diffusive CH₄ flux reported by Gorham (1991) (~4 g m⁻² yr⁻¹).

Although natural peatlands are a significant source of CH₄, they also store large amounts CH₄ held as entrapped gas (Fechner-Levy and Hemond, 1996; Glaser *et al.*, 2004; Strack *et al.*, 2005). Current predictions for climate change suggest a reduction in CH₄ flux from northern peatlands, and increased CO₂ fluxes. However, if episodic

release of these gas stores is considered, it could significantly offset the predicted reductions in CH₄ release (Roulet *et al.*, 1992; Strack *et al.*, 2005) and very possibly exceed it.

1.3 Objectives

While research examining entrapped gas and ebullition processes has increased recently, there remains a relatively poor understanding of these processes and the interconnection of ebullition and entrapped gas with other peatland processes. Indeed current research suggests that a better understanding of these processes is needed as they may have significant impacts on how many peatland processes are understood and measured (e.g. Kellner *et al.*, 2004; Strack *et al.*, 2005; Kellner *et al.*, 2005).

Research to date has generally reported entrapped gas from incubated peat cylinders as changes over the experimental period or as total volumes at the onset and completion of study (e.g. Beckwith and Baird, 2001; Baird and Waldron, 2003; Baird *et al.*, 2004; Kellner *et al.*, 2005), but has not examined the variability of entrapped gas within the cylinders, or the degree to which these fluctuations could impact other processes. Similarly, although the existence of an entrapped gas threshold has been suggested and peat structure has been implicated in establishing it (Baird *et al.*, 2004, Kellner *et al.*, 2005), to date no work has been published examining indicators of peat structure in relation to entrapped gas volume development, and the occurrence and characteristics of ebullition events. In contrast, although the relationship between periods of decreasing

atmospheric pressure and ebullition occurrence has been well established in literature for both field (e.g. Fechner-Levy and Hemond, 1996; Glaser *et al.*, 2004) and laboratory (e.g. Tokida *et al.*, 2005b; Kellner *et al.*, 2006) experiments; there appears to be no work examining what characteristics of falling pressure contribute to this relationship or how they influence ebullition event characteristics. Laboratory measurement of ebullition events have used various incubation temperatures (e.g. Reynolds *et al.*, 1992; Baird *et al.*, 2004; Kellner *et al.*, 2006), however there also hasn't been a direct comparison between cylinders at multiple incubation temperatures within the same experiment making it difficult to directly compare the effect of temperature on entrapped gas and ebullition processes.

Consequently, understanding entrapped gas variability, gas threshold development and the relationship between falling atmospheric pressure and ebullition are of key importance in determining how entrapped gas volumes and ebullition events affect the hydrologic, biogeochemical and ecological functions of peatlands, and the temporal variability of those effects. The aim of this thesis therefore, is to develop a better understanding of entrapped gas and ebullition processes and the interactions of these processes with other peatland processes by examining entrapped gas variability, peat threshold indicators and the nature of the relationship between falling atmospheric pressure and ebullition. In order to facilitate this research, three main objectives have been identified:

- Examine variations in entrapped gas content in six intact peat cores at three incubation temperatures in order to:
 - Determine the magnitude and frequency of changes in entrapped gas content, and to understand how temperature and atmospheric pressure influence these fluctuations, and
 - Employ an iterative model based on the ideal gas law and Henry's law to estimate changes in entrapped gas content

- Investigate the influence of peat structure on ebullition by:
 - Measuring bulk density as an indicator for peat strength, and
 - Comparing bulk density to measured ebullition data to characterize patterns based on variations in bulk density

- Determine the relative influence of pressure change behaviour on ebullition occurrence and characteristics and to further establish the relationship between ebullition and decreasing pressure by:
 - Comparing measured ebullition data with atmospheric pressure data, and
 - Comparing the statistical importance of various pressure change characteristics on measures of ebullition events.

CHAPTER 2: METHODS

2.1 Experimental design

Dr. Erik Kellner and Marieke Oosterwoud with the assistance of other members of the ecohydrology research group at McMaster University conducted the laboratory experiment in 2004. Data analysis for the purposes of this thesis was completed by the author (Kristen Harrison) in 2005-2006. Six peat cores were removed from the St. Charles-de-Bellechasse peatland in late February 2004 and incubated in the laboratory in sealed cylinders for 172 days at temperatures representative of the range of conditions found in natural peatlands from which the cores were removed. One cylinder was incubated at room temperature (17 - 26 °C, mean = 20°C), representing mid-late summer conditions. Three cylinders were incubated at 11 °C representing late spring, early summer and autumn conditions and one cylinder was incubated between 2 and 5 °C (mean = 4°C) to represent early spring and late autumn conditions. A final cylinder was incubated at room temperature (~20°C) in an unsealed cylinder to ensure that the presence of the end plates was not influencing observations in the sealed cylinders. On experiment day 78 the climate chamber failed causing the 11°C incubation cylinders to temporarily (~12 hours) rise to 41°C and then dropped to room temperature where they were maintained until the end of the experiment.

Volumetric water content (VWC), ebullition volume, ebullition CH₄ concentration, pore-water CH₄ concentration, air temperature and atmospheric pressure were measured throughout the experiment. Details of the study area and methods are presented below.

2.2 Study area

Cores for the experiment were collected from a poor fen located near the village of St. Charles-de-Bellechasse, Québec (46°40'N, 71°10'W), ~25 km southeast of Quebec City. The site is a 3-ha natural remnant within a patterned fen complex that has been subjected to drainage and peat extraction activities over the past decade. Site topography consists of ridge-lawn-pool features with a maximum elevation range of ~60 cm. Vegetation within the site is topography dependent, with small trees (*Larix. spp.* and *Betula. spp.*) located sporadically across the site. Ridge areas are dominated by low ericaceous shrubs, giving way to sphagnum dominated lawns with sparse sedge and grass cover, and finally to floating sphagnum mats surrounding open water pool perimeters. *Sphagnum papillosum*, *S. magellanicum* and *S. majus* dominate the moss layer. Within the vascular plant community, *Rhynchospora alba* and *Carex spp.* are dominant. This site is located within the Low Boreal Wetland Region (NWWG, 2004) and the 30-year (1971-2000) averages for mean daily temperature and precipitation (water equivalent) are 16.5 °C, 89.8 mm and –12.8 °C, 114.2 mm in June and January respectively (Environment Canada, 2004). Peat thickness ranges between 1.0 and 1.2 m across the site.

2.3 Laboratory Experiment

Peat cylinder preparation and design

Peat cores were removed with a chainsaw while the peat was frozen in February 2004 to minimize disturbance to the samples. The cores were transported back to the McMaster Ecohydrology lab, kept frozen in coolers, and transferred to a freezer. Each

core was cut to size and fitted into a PVC cylinder (20cm diameter, 24 cm long). All cores had the growing *Sphagnum* surface removed prior to being fitted into the PVC cylinder. Five cylinders were fitted with two end plates; the sixth was fitted with only one end plate as a control to ensure that the presence of the end plates was not influencing observations in the sealed cylinders.

Each cylinder was fitted with two pore-water sampling ports (silicone tubes attached to stopcocks) and two two-rod, 20 cm Time Domain Reflectometry (TDR) probes in the upper and lower portions of the cylinders. Cylinders fitted with two end plates were connected to gas traps consisting of a tube connected to a bottle with a stopcock, backfilled with water that acted as a siphon, displacing water as gas was released (Figure 2.1). End plates fitted with gas traps were sloped towards the centre, allowing gas to freely enter the gas trap. The cores were then thawed and slowly wetted from the base using de-aired water.

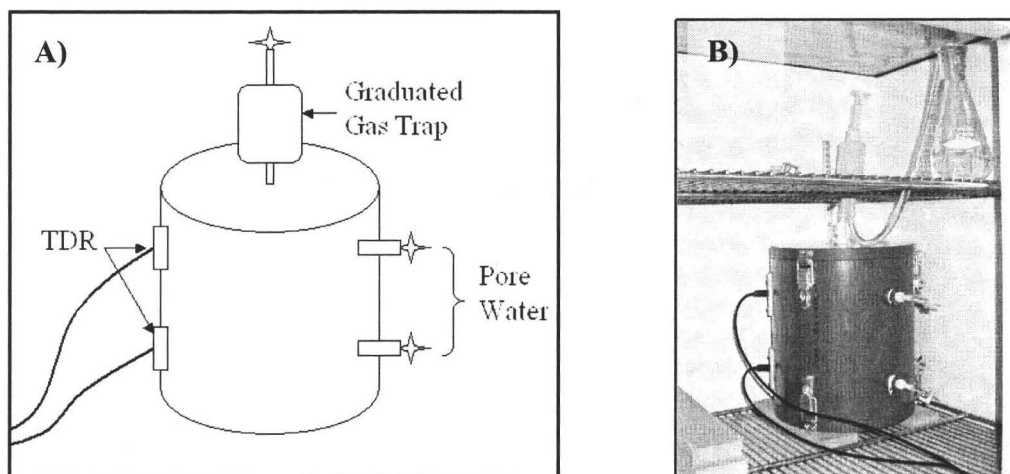


Figure 2.1: Cylinder equipment set-up: A) Illustrative diagram, B) working cylinder set-up. See text for details

CH₄ ebullition and pore-water

The volume of gas collected in the gas traps of cylinders was recorded on a daily or more frequent interval during periods of high activity. When sufficient gas volumes had collected (greater than 3 ml) the entire volume was removed for analysis using a syringe. 1 ml of this gas was transferred to a clean 10 ml syringe, and backfilled with 9 ml N₂. After preparation, these samples were analyzed on a gas chromatograph (GC) (see below). Ebullition was then converted to flux values (mg m⁻² d⁻¹). Ebullition was also converted to volume of CH₄ (ml) and percent CH₄ by volume was calculated. Pore-water samples were collected via the two pore-water ports located in each cylinder twice weekly. From both the upper and lower ports, 5 ml samples were removed using clean 10 ml syringes. The pore-water samples were then backfilled with 5 ml N₂ and shaken for 10 minutes, allowing CH₄ dissolved in the water to move out of solution and into the headspace. The headspace was subsequently transferred to a clean 10 ml syringe and analyzed on a GC. All gas samples (ebullition and pore-water) were analyzed for CH₄ content using a Varian 3800 GC with a Porapak N column at 50 °C and flame ionization detector (FID) at 250 °C with helium carrier gases at a flow rate of 30 ml/min. The GC was calibrated using a 2500 ppm CH₄ standard.

Entrapped gas content

Entrapped gas content was calculated using measured ‘saturated’ volumetric water content every four hours local standard time (LST) using the Campbell Scientific Inc.

TDR 100 and logged on a Campbell Scientific CR10x data logger. Using methods developed by Kellner and Lundin (2001) TDR data was converted into volumetric gas content (VGC) data as given by:

$$VGC = \frac{V_g}{V_t} \quad [3]$$

where V_g is the volume fraction of entrapped gas and V_t is the total volume of the peat sample (gas + water + peat fibres). For the duration of this thesis, the symbol V_g is in reference to the volumetric gas content calculated according to the above equation represented as either an integer of less than 1, or as a percentage (e.g. $V_g = 0.08 = 8\%$).

Atmospheric pressure and temperature

Atmospheric pressure (mbar) was measured within the laboratory every ten minutes at LST with a RM Young 61208V Barometric Pressure Sensor mounted to a board open to the air. Pressure data collected within the lab was converted from mbar to kPa for comparison to outdoor atmospheric pressure (kPa) measured at the Hamilton International Airport ~20km south-east of the lab (Environment Canada, 2004), to test the accuracy of the data, and also to examine any discrepancy between outdoor and room atmospheric pressure. Air temperatures of the peat cylinders ($^{\circ}\text{C}$) were measured every four hours (LST) using copper constantan thermocouples located in each incubation area. In-lab atmospheric pressure (mbar) and temperatures ($^{\circ}\text{C}$) were logged on a Campbell Scientific Inc. CR10x data logger with AM16/32 multiplexer.

Bulk density

Following the experiment, cylinders 1, 2, 3, 4, and 5 were frozen and cut into five 4 cm thick layers (centred at 2, 6, 10, 14, and 17 cm depth); each layer was then subdivided into 9 sections. Segments were dried at 75°C for 48 hours, dry weights (g) were then recorded (peat only) and bulk density was calculated using [4]:

$$BD = \frac{\text{DryPeatWeight}(g)}{\text{SegmentVolume}(cm^3)} \quad [4]$$

Average bulk density values were calculated for each layer (depth) and the upper and lower cylinder portions to coincide with equipment placement. Bulk density for cylinder 6 was not determined following the experiment, and the core was not later available for processing.

2.4 V_g variability

CH₄ equilibrium aqueous phase concentrations

Potential equilibrium aqueous phase concentrations (EAPC) for CH₄ were calculated to evaluate the relative potential difference of EAPC for CH₄ between incubation temperatures and the two instrumentation depths. EAPC values were calculated using alpha (α) solubility values from Lange's Handbook of Chemistry (Dean, 1999), with Henry's law constants calculated according to:

$$H_d = \frac{\alpha}{R} \quad [5]$$

where α is the volume of gas (ml) dissolved in 1 ml water at 1 kPa at a given temperature ($^{\circ}\text{C}$) and R is the Ideal gas law converted to $^{\circ}\text{C}$ (Dean, 1999). Henry's law constants were calculated at 1°C increments/intervals for temperatures 0°C - 30°C . Calculation intervals above 30°C were reduced to every 5°C up to 50°C , this is reduced as temperatures only exceeded these levels during the over-heating of the climate chamber that occurred on day 238 and are excluded from data analysis, excluding the modeling.

EAPC values for CH_4 were calculated based on two headspace scenarios (100% CH_4 , 20% CH_4), two bubble diameters (0.01 cm, 0.00001 cm), and two locations within the cylinders (upper and lower TDR locations, 3.5 and 18.5 cm below the peat surface respectively). EAPC values were calculated for the 100% CH_4 scenario using:

$$EAPC_{100\%CH_4} = H_{d_t} \cdot P_{tot} \cdot 1000 \quad [6]$$

where H_d is the Henry's law constant for CH_4 at time-step t , and P_{tot} is total pressure which is the sum of atmospheric pressure at time-step t , hydrostatic pressure and excess pressure from the bubble radius, the latter two being constant for each time-series set of calculations. EAPC values for the 20% CH_4 scenario are calculated using:

$$EAPC_{20\%CH_4} = H_{d_t} \cdot (P_{tot} - P_{w.v.sat} - 0.8 \cdot P_{atm}) \cdot 1000 \quad [7]$$

where pressure is represented as total pressure minus the water-vapour saturation pressure at time t and the partial pressure of 80% nitrogen in the headspace. Water vapour saturation pressures at 2°C intervals are used. Measured temperature and atmospheric

pressure values from the experiment are used for calculating EAPCs at each 4-hour measurement interval.

V_g variability model

Changes in V_g according to the Ideal gas law (IGL) and Henry's law (HL) were calculated using Equations [1] and [2] using methods presented by Kellner *et al.* (2006). Solubility (H_d) varies between gas species such that changes in temperature and or atmospheric pressure affects partitioning between the aqueous and gaseous phases differently for each species. As such, Equations [1] and [2] cannot be used in their presented form to calculate changes in V_g . Rather, IGL and HL are dealt with separately in an iterative scheme, considering changes in partial pressures and dissolved concentrations for each gas species (CO_2 , N_2 , CH_4) to generate volume changes for the gaseous phase of each. The sum of changes generated by IGL and HL for all species are then combined to give ΔV_g . A linear relationship for solubility is assumed where $H_{d,i} = k_i T + m_i$ where k_i and m_i are parameters representing changes in solubility with respect to temperature and pressure respectively for each gas species.

To accommodate for biogenic gas production in the cylinders, a bulk gas production term was added incorporating production of all gas constituents minus losses (e.g. oxidation), and is assumed added in the gaseous state. Production values are adjusted based on incubation temperature (4°C, 11°C and 20°C) and model fit for each cylinder (C1, C3-C6), and compared against literature values. Pressure, temperature and ebullition data from the laboratory experiment were used for the model.

Where Kellner *et al.* (2006) employed a gas threshold to model ebullition events based on changes in V_g , this work models V_g variability by using forced ebullition events based on observed events (time of occurrence and volume) applied to the corresponding time-step in the model. Model predictions were compared with measured V_g from the laboratory experiment (see above).

2.5 Atmospheric pressure and ebullition relationship

Atmospheric pressure data was subdivided into periods of increasing and decreasing pressure (herein referred to as ‘pressure periods’). Based on these periods ebullition events were then subdivided so that each event was associated with a specific pressure period. For each decreasing period, the magnitude (M), duration (D) and rate (R) of decrease was determined. Within each pressure period, average ebullition characteristics (total volume, average flux, and average percent CH₄ by volume) were determined for each cylinder (C1, C3-C6) and for all cylinders combined.

Regression analyses were conducted using the pressure characteristics as independent variables, and the ebullition characteristics as dependent variables. Each independent variable was tested individually against the dependent variables to test for significant relationships. Results with confidence intervals of 90% or greater were deemed significant.

The relative influence of each independent variable was tested by evaluating each unique combination of these variables (DM, DR, MR, DMR) for relative significance in predicting each dependent variable.

CHAPTER 3: ENTRAPPED GAS AND POREWATER: RESULTS AND DISCUSSION

3.1 Results

Peat characteristics

Bulk density provides a good estimate of the ability of peat to trap gas. Values ranged between 0.024 and 0.156 g cm⁻³ in the peat samples in this study. C3 had the highest average bulk density (0.079 g cm⁻³), followed by C1, C2, C5 and C4 with average bulk densities of 0.074, 0.072, 0.060 and 0.051 g cm⁻³ respectively (Table 3.1).

Bulk density increased with depth in cylinders 1, 3 and 5 with a small decrease at 17cm (Figure 3.1). Bulk density was greatest at a depth of 10-14 cm for these cylinders. C1 had the most prominent increase in bulk density at 14 cm, and contained the highest bulk density values measured of all cylinders. Cylinders 2 and 4 showed greater uniformity in bulk density with depth. Smaller fluctuations in bulk density are more dispersed throughout the cylinders, with C2 having consistently higher bulk densities at each depth. The densest layers in C2 and C4 occurred at two depths, 2 and 17 cm (0.076 g cm⁻³) for C2, and 6 and 17 cm (0.055 g cm⁻³) for C4. Variations in bulk density generate variation in the ability of peat to trap and store gas, such that layers of higher bulk density may act as confining layers, restricting gas movement relative to surrounding areas of lower bulk density.

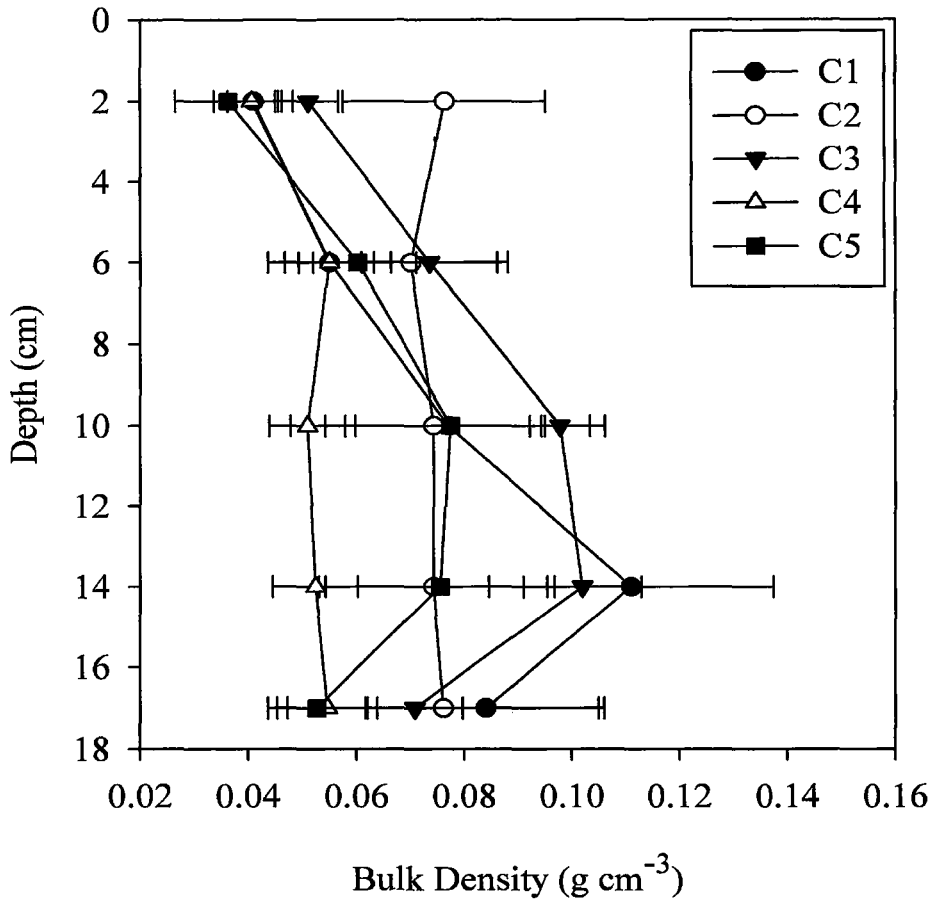


Figure 3.1: Cylinder bulk densities with depth from the peat surface and one standard deviation error bars.

Table 3.1: Bulk density (g cm⁻³) averages for upper and lower portions of each cylinder.

Bulk Density	C1	C2	C3	C4	C5
Upper	0.056	0.073	0.072	0.049	0.056
Lower	0.093	0.075	0.085	0.053	0.063

Pore-water CH₄ concentrations

During the 11°C incubation period (prior to the climate chamber failure), C3, C4 and C5 showed a relatively steady increase in pore-water concentrations with average rates of increase of 0.04, 0.02, and 0.04 mg l⁻¹ d⁻¹. Following failure of the climate chamber to the 20°C incubation temperature, accumulation of CH₄ in pore-waters increased to 0.06, 0.06 and 0.05 mg l⁻¹ d⁻¹ for C3, C4 and C5 respectively. C1 and C2 showed higher initial rates of increase at 0.22 and 0.27 mg l⁻¹ d⁻¹, respectively. After this initial period of increase however, pore-water concentrations appeared to level off on day 250 (C1) and 275 (C2), respectively, fluctuating around means of 11.0 and 12.3 mg l⁻¹ for C1L and C1U respectively; and 13.0 mg l⁻¹ for both C2L and C2U for the remainder of the experiment (Figure 3.2). Similarly, C6 (4°C) showed an increasing CH₄ pore-water concentration of 0.02 mg l⁻¹ d⁻¹ until approximately day 80, after which accumulation slows to be almost negligible for the remainder of the experiment.

Minimum concentration values occurred within a relatively narrow range between 0.1 and 1.9 mg l⁻¹ (Table 3.2) occurring near the beginning of the experiment. Maximum pore-water concentrations occupied a wider range of values between 1.9 mg l⁻¹ in upper portion of C6 (C6U) and 40.7 mg l⁻¹ in the lower portion of C1 (C1L). Dissolved CH₄ concentrations differed between the upper (U) and lower (L) portions of the cylinders. The lower portion of the cylinders contained higher concentrations of dissolved CH₄ than the upper portion with the exception of C3 during the 11°C incubation period and C2, in which the upper portions were slightly higher (Table 3.2).

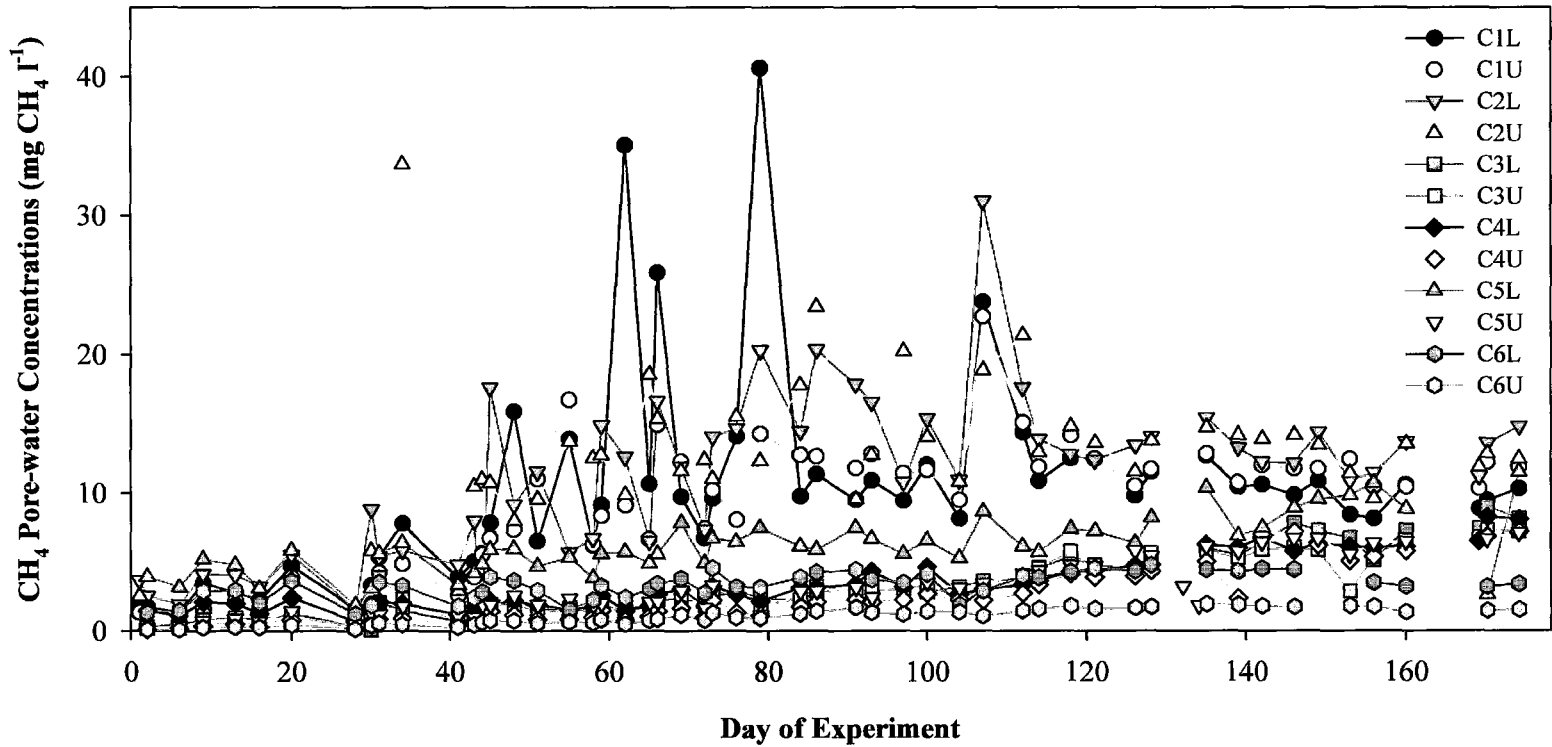


Figure 3.2: CH₄ pore-water concentrations for the upper (U) and Lower (L) portions of each cylinder in mg CH₄ l⁻¹

Table 3.2: Pore-water CH₄ concentration values for each cylinder at both the upper and lower probe locations.

Cylinder	Temperature	Probe	CH ₄ Pore-water concentration (mg l ⁻¹)		
			Average	Minimum	Maximum
C1	20°C	Upper	9.1	0.4	22.7
		Lower	10.1	1.3	40.7
C2		Upper	11.6	0.6	33.7
		Lower	11.2	0.8	31.0
C3*		Upper	4.6	1.9	7.3
		Lower	5.1	2.2	9.0
C4*		Upper	4.0	1.1	7.1
		Lower	4.9	2.2	8.3
C5*		Upper	4.6	1.1	7.1
		Lower	7.5	2.7	11.5
C3	11°C**	Upper	1.5	0.2	3.9
		Lower	1.4	0.1	2.9
C4		Upper	1.0	0.1	2.2
		Lower	1.9	0.7	3.2
C5		Upper	1.6	0.2	3.3
		Lower	5.0	1.9	7.8
C6	4°C	Upper	1.0	0.1	1.9
		Lower	3.3	1.2	4.8

* C3, C4, C5 in the 20°C incubation period is measured after experiment day 78 of the experiment (following failure of the climate chamber)

** C3, C4, C5 in the 11°C incubation period is measured prior to day 78 of the experiment (prior to the failure of the climate chamber)

While pore-water concentrations were largest in cylinders incubated entirely at $\sim 20^{\circ}\text{C}$, CH_4 EAPC values were highest for the $\sim 4^{\circ}\text{C}$ incubation, decreasing with increasing temperature (Table 3.3).

Table 3.3: Theoretical CH_4 equilibrium aqueous phase concentrations (EAPC) (mg l^{-1}) for two bubble diameters (0.00001 cm and 0.01 cm) for each incubation temperature (20°C , 11°C , and 4°C) and for each scenario (100% CH_4 and 20% CH_4 where the balance is N_2 and water vapour) are shown.

Scenario	Section	$\sim 20^{\circ}\text{C}$		$\sim 11^{\circ}\text{C}$		$\sim 4^{\circ}\text{C}$	
		0.00001	0.01	0.00001	0.01	0.00001	0.01
100% CH_4	Upper	25.26	22.16	31.65	27.73	38.02	33.36
20% CH_4 (N_2 , w.v.)		7.09	3.99	9.14	5.22	11.32	6.65
100% CH_4	Lower	25.42	22.32	32.06	28.14	38.77	33.60
20% CH_4 (N_2 , w.v.)		7.26	4.16	9.55	5.63	11.56	6.90

Theoretical CH_4 equilibrium aqueous phase concentration (EAPC) values (Table 3.3) indicate that concentrations in lower portions of the cylinders are slightly larger than upper portions due to increased pressure from overlying materials, however the difference is relatively small with an average increase in EAPC of only 0.4 mg l^{-1} for the lower probe location with a range of $0.2 - 0.6 \text{ mg l}^{-1}$ (data not shown). Pore-water CH_4 concentrations were well below the 20% CH_4 EAPC scenario values (Table 3.3) at the beginning of the experiment. As concentrations increased, all cylinders, with the exception of C6 exceeded this 20% CH_4 EAPC. The 20% CH_4 EAPC was exceeded by the lower portions of C1, C2, C4 and C5, on days 180, 169, 286 and 169, respectively,

and later on days 191, 190, 295, and 278 by the upper portions of these cylinders. The 20% EAPC was exceeded on day 278 for both the upper and lower portions of C3.

The 100% CH₄ EAPC scenario represents a theoretical maximum concentration using recorded atmospheric pressure and temperature conditions. Maximum pore-water values for C3, C4, C5, C6 and C1U remained below this upper limit. C1L and both C2 probe locations had maximum values exceeding the theoretical maximum 100% EAPC values during the experiment. For example, C1L exceeded the theoretical maximum on days 222, 226 and 239 with values of 35.1, 25.9 and 40.7 mg l⁻¹ respectively. C2U and C2L exceeded maximums on days 194 (33.7 mg l⁻¹) and 267 (31.1 mg l⁻¹) respectively.

Concentrations of CH₄ in ebullition gas from C1 had similar patterns to pore-water concentrations over the course of the experiment. C1 showed an initial increase in concentration from the initiation of ebullition events (day 15) to approximately day 80, after which gas concentrations were highly variable around an average of ~45% over the experiment (Figure 3.3). Patterns in C3, C4 and C5 were more difficult to determine as ebullition commenced only after removal from the climate chamber to the 20°C incubation temperature, on day 79 for C3, and 110 for C4 and C5. Nevertheless, similar to C1, they showed a general increase in CH₄ concentrations from ebullition onset, however did not level out before the completion of the experiment (Figure 3.3). C6 did not display any ebullition activity.

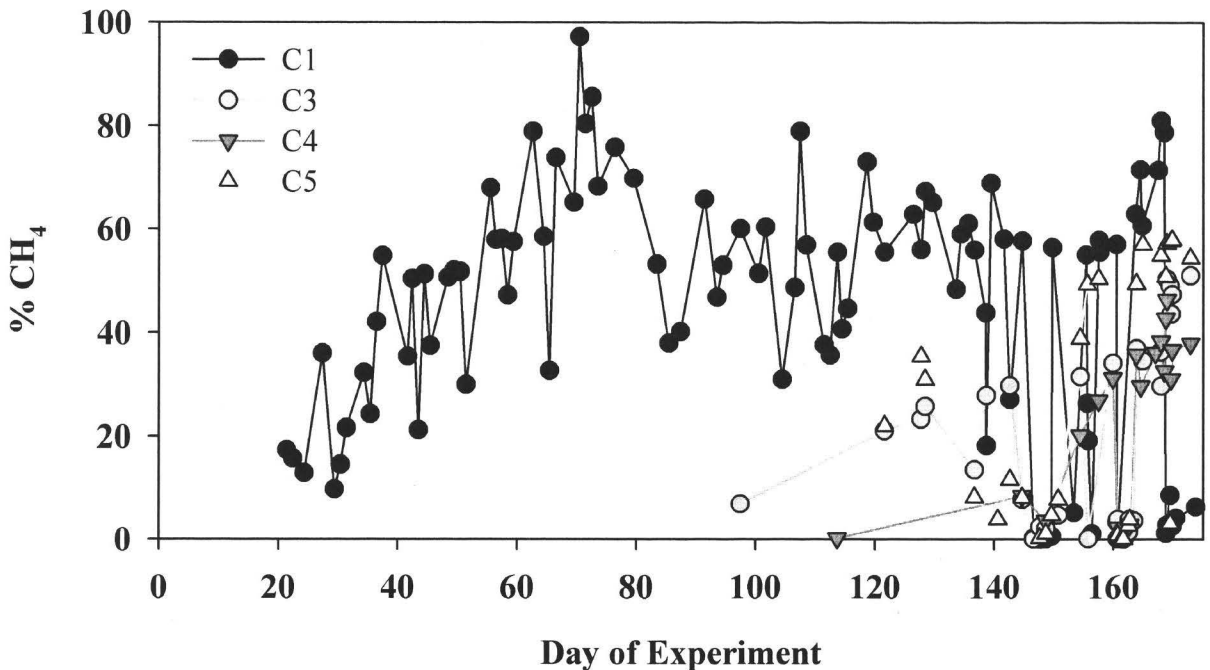


Figure 3.3: CH₄ concentrations (%CH₄) in ebullition gas (shown as percent CH₄) by volume.

Entrapped gas content

As mentioned earlier, the climate chamber housing C3, C4 and C5 at 11°C failed and overheated on Day 78. This sudden rise in temperature is reflected in a spike in gas content in these three cylinders (Figure 3.4). Following this, C3, C4 and C5 were incubated at room temperature (~20°C) with C1 and C2 for the remainder of the experiment. C1 and C2 were incubated at ~20°C and C6 at 4°C for the duration of the experiment.

Initial wetting of the cylinders resulted in air entrapment with initial entrapped gas (V_g) values of between 2 and 9% (Table 3.4). Similar patterns in V_g are displayed by the upper and lower probes of C1 and C2 (20°C), where there is a steady increase in V_g followed by a period of relative stability (Figure 3.4). Average rates of accumulation were calculated for each cylinder from experiment onset to day 78 when C3, C4 and C5 were removed from the 11°C incubation and rates of increase from day 79 to the end of the experiment and are presented in Table 3.5.

Table 3.4: Initial gas contents following wetting at experiment onset by cylinder and probe location.

Probe	Initial Entrapped Gas Content (%)					
	C1	C2	C3	C4	C5	C6
Upper	4	4	7	4	6	3
Lower	9	2	4	7	2	6

Table 3.5: Average rates of accumulation in V_g for the period prior to climate chamber failure (day 78) and following failure (day 79) to the end of the experiment. Calculated as the slope of the line between average gas contents, these values represent an average rate of accumulation for these cylinders.

Period (day)	Rate of Accumulation (ml gas d ⁻¹)											
	C1		C2		C3		C4		C5		C6	
	L	U	L	U	L	U	L	U	L	U	L	U
4-78	9	11	8	11	1	2	2	1	1	1	1	0.0
79-172	0.3	3	4	1	11	2	8	7	10	6	4	0.5

Following the initial decrease in V_g after wetting, C1 and C2 show the fastest accumulation in entrapped gas content (Table 3.5). Rates are slower in C3, C4, C5 and C6 for the initial period of the experiment but are similar, between 0-2 ml gas d⁻¹ (day 4-78). C1 and C2 both show large decreases in the rate of accumulation of gas from days 79-172. Following from the failure of the climate chamber (day 79-172) C3, C4 and C5

showed large increases in their rates of gas accumulation at all probe locations with the exception of C3U where there was no apparent change in accumulation rate (Table 3.5). C6, maintained at 4°C, showed a small increase in accumulation rate in the later period of the experiment, but maintained a slow rate of gas accumulation throughout the experiment.

Measured gas contents at all probes in cylinders 1 and 2 appear to reach a state of relatively constant V_g around which they fluctuate, although each reaches this point at different dates during the experiment, approximately day 30 and 80 for C1L and C1U, and approximately day 115 and 60 for C2L and C2U, respectively (Figure 3.4). The relatively stable nature of these periods is reflected in the decrease in the rates of accumulation indicated in Table 3.5 for days 79-172. C3U also appears to reach a similar state of stable gas content after warming to 20°C on approximately day 120. This pattern is not clearly evident at C3L, or probes in C4, C5, or C6 (Figure 3.4).

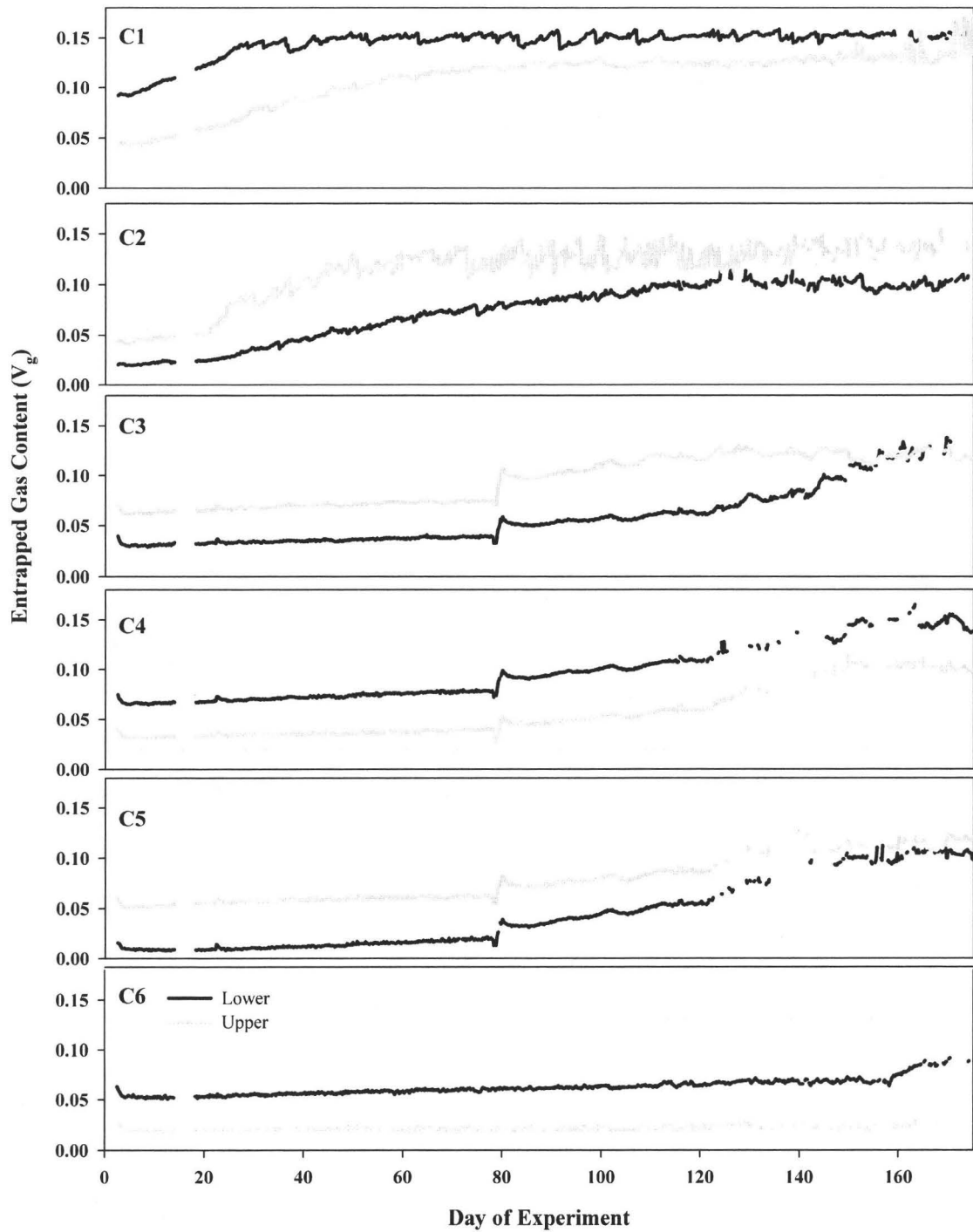


Figure 3.4: TDR-measured entrapped gas content for all cylinders. C3, C4 and C5 are shown across the change in incubation temperature from 11°C (up to day 78) and 20°C for the remainder of the experiment.

To facilitate comparison, entrapped gas contents were examined as the cumulative change in entrapped gas (ΔV_g) (Figure 3.5) for each cylinder. Similar patterns were evident in ΔV_g for all plots of V_g with the exception of C2U. Measured V_g for C2U shows a similar pattern to both C1 probes (U&L) and C2L (Figure 3.4), where there is an increase in V_g until reaching a stable gas content around which it then fluctuates. When examined as the cumulative change in entrapped gas content (ΔV_g) however, C2U does not maintain this pattern. The initial increase in ΔV_g for C2U is evident (Figure 3.5), however it showed only short stable period (~30days) followed then by a decrease in ΔV_g . This indicates that there was no net increase in entrapped gas content over the experiment, however a net increase in entrapped gas content is evident in the measured V_g for this probe (Figure 3.4). C2L increases steadily until approximately day 140 after which it levels off around a ΔV_g of 9%. C1 appears to reach a relatively steady gas content, fluctuating around a mean ΔV_g of ~7 and ~3 % on day 90 and 45 respectively for the lower and upper probes. C2L appears to reach a similar state on day 135 at ΔV_g of ~9% (Table 3.6). To the end of the 11°C incubation period cylinders 3, 4 and 5 showed a steadily increasing ΔV_g , however at the time of climate chamber failure, C3, C4 and C5 had just recovered from the initial drop in V_g noted at the beginning of the experiment. Following failure of the climate chamber to the 20°C incubation temperature ΔV_g increased more rapidly in all three cylinders. Unlike the cylinders at 11°C (C3, C4, C5), C6 at 4°C had not yet recovered from the initial decrease in gas content at the beginning

of the experiment by day 78, however, ΔV_g in C6 steadily increased for the duration of the experiment.

Table 3.6: Cylinder change in entrapped gas content (ΔV_g) by incubation temperature and probe location.

Cylinder	Temperature	Section	ΔV_g (%)	Average ΔV_g (%)
C1	20°C	Lower	4	8.2
		Upper	12	
C2**		Lower	9	5.6
		Upper	2	
C3*		Lower	5	4.1
		Upper	2	
C4*		Lower	4	3.5
		Upper	3	
C5*		Lower	6	4.8
		Upper	4	
C3	11°C*	Lower	0.2	0.2
		Upper	0.3	
C4		Lower	0.5	0.2
		Upper	0.0	
C5		Lower	0.8	0.3
		Upper	-0.1	
C6	4°C	Lower	2	1.4
		Upper	0.6	

** C2U is calculated using V_g values

* C3, C4 and C5 are calculated based on incubation periods: 1) days 0-78: prior to climate chamber failure, 2) days 79-172: post failure of the climate chamber to 20°C

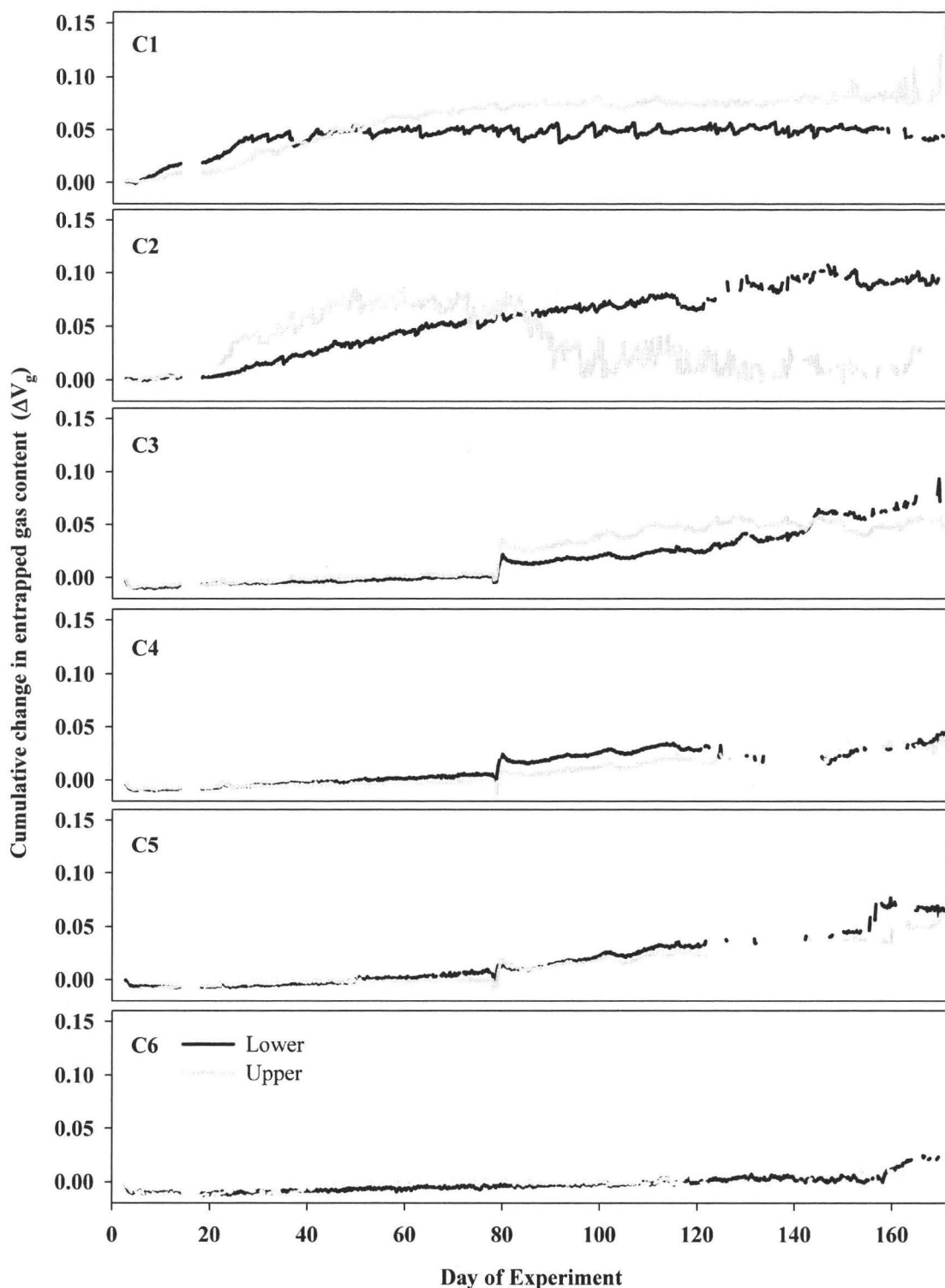


Figure 3.5: Cumulative change in entrapped gas (ΔV_g) generated from TDR-measured gas contents for Upper (grey) and Lower (black) portions of each cylinder.

3.2 Discussion

Effect of capping cylinders

C2 was incubated as a control with no lid to investigate the effects capping the cylinders may have on processes occurring within the cylinders. The concern was that the lids could constrain the encased peat and entrapped gas, potentially increasing pressure within the cylinders, which could result in increased dissolution of gas, reflected as an increase in pore-water CH₄ concentrations, and therefore a decrease in entrapped gas content. The overall effect would be to make a more conservative estimate of entrapped gas, but to potentially over-estimate dissolved concentrations. To test the effect of the lids, only C1 and C2 can be directly compared as they were incubated under the same conditions.

Comparison of pore-water CH₄ concentrations from C1 and C2 (Table 3.2) shows that C2 has the higher pore-water concentrations, although still within a similar range as C1. This seems to indicate that there is no large increase in the dissolved phase related to increased pressure within the cylinders capped with lids. Similarly examination of measured V_g within these cylinders (Figure 3.4) shows similar patterns and entrapped gas contents between these two cylinders. If there were a significant increase in pressure a decrease in entrapped gas content in C1 compared to C2 would be expected.

Fluctuations in V_g are larger throughout much of the experiment for C2U, however similar fluctuations were recorded in C1L later in the experiment, and as such,

these are not considered a direct effect of the lid. Attention should be drawn to the pattern of C2U ΔV_g (Figure 3.5), which shows a distinct difference from other cylinders. These are suggested to be an artefact of the large fluctuations and small gaps in data seen at this probe as this loss in entrapped gas is not evident in the plot of V_g for C2U, and C2L shows a pattern similar to those found in other cylinders (Figure 3.4). Further investigation of this pattern in future work should be considered to verify that this is not an effect of the lids. Given the supporting evidence of pore-water concentrations and V_g , the lids are not considered to have a large influence on the processes investigated in this thesis and C2 is not further considered in this thesis.

Gas phase establishment

Bubble formation by nucleation in a fully saturated medium requires that the partial pressures of dissolved gases exceed the hydrostatic pressure in the media in which they occur (Rothfuss and Conrad, 1998). However, once a gas phase exists, transfer between the dissolved and gaseous phase is controlled by Henry's Law (Strack *et al.*, 2006), therefore allowing the gas phase to increase at concentrations below EAPC values.

Upward wetting has been employed in several biogenic gas studies (e.g. Beckwith and Baird, 2001; Baird and Waldron, 2003; Baird *et al.*, 2004; Kellner *et al.*, 2006) with resulting entrapped air content in cylinders of between 1-13% (Beckwith and Baird, 2001; Baird *et al.*, 2004; Kellner *et al.*, 2006). Similar to other studies, initial air content following upward wetting for all cylinders in this experiment was between 2 and 9 %.

This evidence of consistent under-saturation with respect to water suggests that a gas phase is consistently present at shallow depths. As such, Henry's law would control gas transfer, allowing entrapped gas contents to increase without exceeding EAPC values for a given set of conditions (pressure and temperature).

Following wetting, entrapped gas contents showed a slight decrease as the entrapped air partially dissolved into the de-aired water used to saturate the cylinders. Following this initial drop, biogenic gas content within all cylinders in this experiment, regardless of incubation temperature, increased when pore-water concentrations were below EAPC values. As such, it is unlikely that initial bubble formation by nucleation above a given EAPC value would be required to initiate gas phase development in the cylinders from this experiment. Over the course of the experiment cylinders 1 and 2 (20°C), and 3, 4 and 5 when incubated at 20°C exceeded their calculated EAPC values with no marked increase in entrapped gas formation, supporting evidence for earlier establishment of a gas phase. In the final cylinder, C6 (~4°C) where EAPC values were never exceeded, a continuous accumulation of gas was evident. These observations support work by Baird *et al.* (2004) in which they challenged the development of bubbles only above a dissolved concentration threshold, finding that gas accumulation occurred at pore-water concentrations prior to reaching and well below the limit currently used in peatland ebullition models (e.g. Walter *et al.*, 1996; Walter and Heimann, 2000; Granberg *et al.*, 2001). Given the evidence presented by Baird *et al.* (2004) and supporting findings from this experiment, it appears that consideration must be given to the effects of air entrapment in shallow peat in models that account for the presence of entrapped gas in

peat. Only using nucleation for gas development does not satisfactorily represent bubble formation in shallow peat as it assumes an initial state of full saturation. At depths generally unaffected by water table fluctuations and precipitation infiltration for air entrapment, nucleation may be a major avenue for bubble formation, and as such may be of increasing importance with depth in the peat profile.

Ponded infiltration and upward wetting are the closest approximation to natural infiltration and water table fluctuation events in natural shallow peat environments. It is probable that laboratory wetting methods generate lower degrees of air entrapment than natural wetting events (Beckwith and Baird, 2001) and as such, we can assume that shallow depth air entrapment occurs in natural peatland systems. The volume of entrapped gas in natural systems undergoes significant seasonal variation caused predominantly by large changes in EAPCs and production rates and changes in response to interannual variability in climatic conditions. In the event that during some period (e.g. winter), the gas phase is eliminated, the first infiltration event or water table rise would trap air, re-establishing the control of Henry's law on phase transfer of gas within shallow peat. In deeper peat and in the event that this does not occur in shallow peat, accumulation of the dissolved gases and nucleation could re-establish a gas phase. It is highly likely that small bubbles remain trapped within or attached to peat fibres throughout seasonal fluctuations in entrapped gas, maintaining a gas phase at some level.

The accumulation of gas at low temperatures and below EAPC values suggests that there is potential for gas accumulation to occur in cold environments where these

processes are active, but slow. Walter *et al.* (2006) found ebullition to be of significant importance in Siberian lakes as a source of CH₄, finding point sources of ebullition and also ebullition ‘hotspots’, which were sufficiently active to prevent ice formation through the winter. Given this, we might expect to find active gas and ebullition processes in sub-arctic peatlands, although we could expect their activity to be slowed compared to those in warmer environments.

Gas distribution and bulk density

Cylinders maintained at ~20°C reached a relative ‘steady state’ in entrapped gas content (V_g); a pattern not clearly evident in any other cylinders during the experiment. This pattern in V_g has been observed in numerous other studies including Beckwith and Baird (2001), Baird *et al.* (2004), Strack *et al.* (2005) and Kellner *et al.* (2006). Baird *et al.* (2004) suggest that this steady state represents a fuzzy threshold between storage and release of gas in peat related to peat strength and structural characteristics (Johnson *et al.*, 2002; Price, 2003; Baird *et al.*, 2004; Kellner *et al.*, 2006). The gas threshold can be considered the point at which the buoyant forces of the entrapped gas and the restraining forces of the peat are in balance, where an increase in gas will then trigger a release (Johnson, 2002; Kellner *et al.*, 2005). Therefore, given enough time for V_g development, each cylinder would exhibit the characteristic ‘steady’ V_g after reaching its threshold. Bulk density is a good indicator of the ability of peat to trap gas, so that changes in trapping capability will have a very high spatial variability within a peatland both vertically through a profile and horizontally across a site (Belyea and Clymo, 2001). As

such, threshold values are difficult to assign to large areas, but rather are defined on a microtopographic scale and potentially on smaller scales based on smaller peat structures. As such, each location or sample will have a different gas threshold.

Over the relatively small range of bulk densities found in the cylinders, evidence of the influence of bulk density on V_g is relatively limited. The general uniformity of C4 with depth indicates that there are likely minimal differences in gas storage potential with depth related strictly to peat structure. Although both C3 and C5 show a pattern with depth, the difference relative to other layers is not significant enough to establish a relationship regarding bulk density and V_g in any direction. The bulk density profile of C1 however, displays a layer of higher bulk density at 14 cm, just above the lower instrumentation depth and may be a large enough increase to generate a change in storage potential (Figure 3.1). The probes located at C1L show a distinct pattern in V_g of build-up and sudden drops that are not evident in the C1U probe (Figure 3.4). This pattern may indicate the sudden movement of gas within or out of the cylinder. Because this pattern is measured at the probe located below a high bulk density layer may indicate that the higher bulk density peat is acting as a confining layer for entrapped gas in C1. Without other similar bulk density profiles in other cylinders it is difficult to confirm this relationship, but should be a consideration for future work.

Pore-water and gas content

As C3, C4 and C5 warmed from 11°C to the 20°C incubation temperature, the rate of CH₄ accumulation increased, indicating an increase in gas production, as EAPC values

would decrease as temperatures warmed. Dissolved CH₄ concentrations following the switch to the 20°C incubation temperature are lower than those seen in C1 (and C2) stored from experiment onset at 20°C. This may in part be due to a lag in warming of the peat within C3, C4 and C5 to the change in incubation temperature, and a similar lag in response time of gas producing organisms, particularly methanogenic organisms. Although no internal peat temperature data is available, this seems to be a reasonable explanation for the differences observed. Given the shorter periods over which they are incubated at 20°C, it follows that concentrations in C3, C4 and C5 remain smaller than in C1 (and C2) for the duration of the experiment.

Similarities exist between the patterns of V_g and pore-water concentrations (Figures 3.4 and 3.2). Patterns of dissolved concentrations in all cylinders appear to generally agree with the patterns in V_g with the exception including the response of dissolved concentrations in C3, C4 and C5 to failure of the climate chamber, and the periodic over-saturation witnessed in C1 and C2. The non-responsiveness of dissolved CH₄ concentrations to failure and overheating of the climate chamber may in part be due to sampling frequency for pore-water (twice weekly, event was 1 day in duration), but may more strongly indicate that a significant proportion of the change registered by the TDR probes was generated by the thermal expansion of gas present within the system.

Both probe locations in C1 (and C2) develop a relatively stable condition in both V_g (Figure 3.4) and dissolved CH₄ concentration (Figure 3.2) at the similar times during the experiment. The coincidence of these patterns indicates that the entrapped gas and

aqueous phases of the cylinders are in equilibrium with one another, and that the system at these locations has also reached a relative steady-state condition controlling the entrapped gas volume and based on the composition of these gases, their respective dissolved phases.

Concentrations displayed by the 4°C cylinder (C6) and those of C3, C4 and C5 when stored at 11°C are similar. This may be a combination of the increased potential for dissolution at lower temperatures balancing reduced production such that there is little overall difference in observed dissolved concentrations at 4°C and 11°C. Without information regarding production rates in these cylinders however, no further analysis can be done to identify the cause of these similarities.

Implications

While temperature is a major control on gas production, it is probable that the subsequent distribution of entrapped biogenic gas within peat is more closely associated with variations in bulk density (Rothfuss and Conrad, 1998; Romanowicz *et al.*, 1995; Kellner *et al.*, 2005; Tokida *et al.*, 2005b). Gas storage potential changes with variations in bulk density. Given that bulk density generally increases with depth, it would follow that thresholds also increase with depth through the peat profile (Boelter, 1965; Glaser *et al.*, 2004) according to the dominant peat forming vegetation species (Belyea and Clymo, 2001). *Sphagnum* species produce layers of relatively low bulk density in peat compared to sedges, which can form dense root mats and shrubs whose woody roots and stems add significant strength to the peat matrix (Belyea and Clymo, 2001).

This suggests that the development history of a peatland is important for controlling gas storage and release. This could then be related to the distribution and evolution of microforms across peatlands dominated by hollow-lawn-hummock patterning (Belyea and Clymo, 2001). Dry areas, dominated by sedges and shrubs will likely develop confining layers with high bulk densities, small pores thus, higher capillarity, and therefore an increased ability to constrain gas (Johnson *et al.*, 2002; Price, 2003, Glaser *et al.*, 2004), which in turn decreases hydraulic conductivity. A reduction in hydraulic conductivity reduces water losses from the peatland so that over time, these areas may be able to moderate their moisture conditions, becoming wetter. Conversely, wet areas dominated by *Sphagnum* produce layers that do not readily trap gas, with low peat ‘strength’, large pore spaces and therefore weaker capillary forces and a resultant decrease in gas storage potential (Johnson *et al.*, 2002; Price, 2003).

As moisture conditions change, vegetation cover responds with each new layer in the profile corresponding to these fluctuations (Belyea and Clymo, 2001) and subsequently will influence gas storage at that location. Moving through the peat profile, a complex system of layers with different structural properties creates a highly variable pattern of gas thresholds across and through a site. Tokida *et al.* (2005b) found a high degree of spatial variability of gas contents across a peatland in Japan, ranging from 0-19 % by volume. These fluctuations in vegetation cover and subsequently the complex gas storage network created, may give peatlands the ability to control moisture conditions to some extent, regulating hydrological function according to variability in entrapped gas content.

CHAPTER 4: BIOGENIC GAS EBULLITION

4.1 Results

Entrapped gas content variability

In addition to the large-scale patterns in V_g discussed in Chapter 3, smaller fluctuations also occur. These intermediary changes in V_g , measured as the change over a period of consistently increasing or decreasing gas content, account for the smaller, more frequent changes in measured V_g data within the larger trend (Figure 4.1). Like the larger patterns in V_g , intermediary fluctuations vary between cylinders and within cylinders at each probe location (Table 4.1). These intermediary changes are examined excluding the initial decrease in V_g due to dissolution of air following initial wetting.

During the 11°C incubation period, C3, C4 and C5 showed similarly sized fluctuations in V_g with maximum intermediary fluctuations of approximately 0.5% and 1% in increasing and decreasing directions respectively (Table 4.1). Average intermediary fluctuations during this period were much smaller, 0.1-0.2%. The magnitude of increasing V_g fluctuations increased at the 20°C incubation temperature with maximum increases ranging from 1.0-1.6%, conversely, there was little change in the magnitude of maximum decreasing V_g fluctuations during the 20°C incubation period. Average fluctuations for C3, C4 and C5 at 20°C also increased to between 0.2 and 0.3 %.

C1 had the largest maximum increasing and decreasing intermediary fluctuations and the largest average fluctuation size, although still relatively similar to C3, C4 and C5 while incubated at 20°C (Table 4.1). C6 (4°C) maximum increase values were larger

than C3, C4 and C5 at 11°C, but generally smaller than those stored at 20°C. This may in part be due to the duration of each period considered, 78 days for C3, C4 and C5 at 11°C, and 172 days for C6 at 4°C. Overall, the range of values for the maximum increase (0.4-4.0%) was larger than the range of values for the maximum decrease (0.7-3.0%), however average fluctuation size is more uniform across the cylinders, ranging from 0.1-0.4%.

Table 4.1: ΔV_g ranges, and variability for all cylinders. Range over which V_g for each cylinder occurs, compared with entrapped gas variability maximums, and range. C3, C4 and C5 at 11°C are for days 4-78 (excludes initial drop in V_g due to dissolution of entrapped air after wetting), and days 79-172 for the 20°C temperature group.

Cylinder	Temp. (°C)	Section	ΔV_g Range (%)	Intermediary Fluctuations (V_g)			
				Maximum Increase* (%)	Maximum Decrease* (%)	Average (%)	Range (%)
C1	20°C	Upper	4	4.0	3.0	0.4	7.0
		Lower	12	1.6	1.9	0.4	3.5
C3		Upper	5	1.2	1.1	0.3	2.3
		Lower	2	1.6	2.2	0.3	3.8
C4		Upper	4	1.0	0.7	0.2	1.8
		Lower	3	1.1	1.0	0.2	2.1
C5		Upper	6	1.2	0.8	0.2	2.0
		Lower	4	1.4	1.0	0.2	2.4
C3	11°C	Upper	0.2	0.5	1.0	0.1	1.4
		Lower	0.3	0.4	1.0	0.1	1.4
C4		Upper	0.5	0.4	1.3	0.2	1.7
		Lower	0.0	0.5	1.0	0.2	1.5
C5		Upper	0.8	0.5	1.0	0.2	1.5
		Lower	-0.1	0.5	0.7	0.1	1.2
C6	4°C	Upper	2	0.7	1.0	0.2	1.7
		Lower	0.6	1.1	1.1	0.2	2.1

Note: all values exclude the initial decrease in V_g and all values are rounded
* for a consistent direction of change (increasing or decreasing)

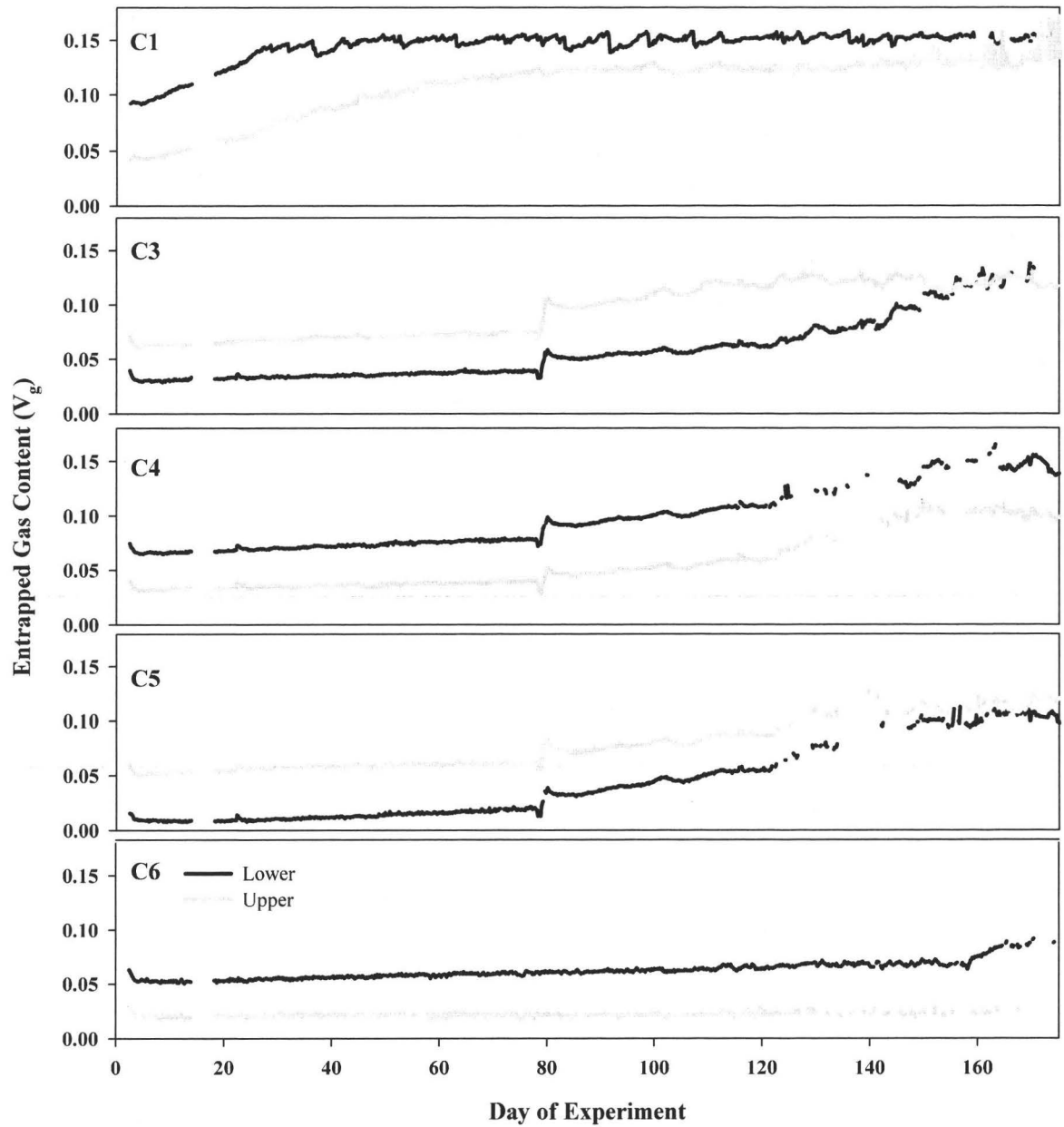


Figure 4.1: TDR-measured entrapped gas contents for Upper (grey) and Lower (black) portions of each cylinder. Note the patterns of increasing V_g in all cylinders. C3, C4, C5 are incubated at 11°C until day 78 and at 20°C from day 79-172.

Ebullition

Ebullition only occurred in the cylinders incubated at 20°C. As such, all analysis regarding ebullition was conducted during 20°C incubation periods: days 0-172 for C1, and days 78-172 for C3, C4 and C5. Ebullition in C1 began on day 15 of the experiment, after 15 days at 20°C. C3 showed active ebullition after only 1 day at 20°C (day 79 of the experiment) and after 32 days at 20°C (day 110) ebullition initiated for both C4 and C5. C6, incubated at 4°C, showed no signs of active ebullition and is not investigated further in this chapter. C1 had the greatest number of ebullition events (144) followed by C4, C5 and C3 with 86, 81 and 80 events respectively. The onset of ebullition coincided with increases in entrapped gas contents.

Although C1 had the greatest number of ebullition events, when examined as the number of events per day from initial onset of ebullition, C4 had the highest event frequency (1.4 events/day), followed by C5, C1 and C3 with 1.3, 0.9 and 0.9 events/day respectively.

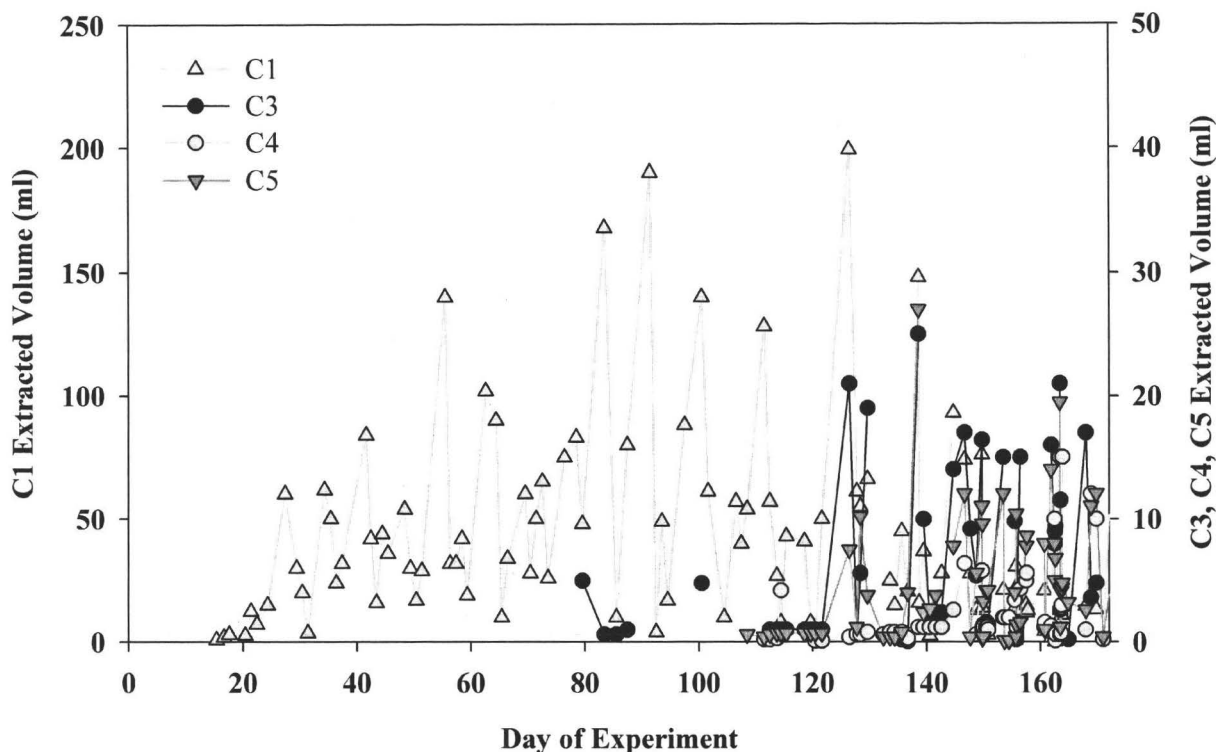


Figure 4.2: Extracted ebullition volumes (ml) for cylinders 1, 3, 4 and 5. C6 showed no signs of active ebullition.

Total and average values for ebullition volume (ml) and CH_4 flux ($\text{mg m}^{-2} \text{d}^{-1}$) reveal that C1 had both the largest volume of gas released via ebullition, and the highest rates of CH_4 flux (Table 4.3). Of those cylinders brought to 20°C on day 78, C3 had the largest average ebullition volume (6 ml) followed by C5 and C4 at 4 and 3 ml respectively. In contrast, when comparing CH_4 flux values the order is reversed where C4 had the highest average at $123 \text{ mg m}^{-2} \text{d}^{-1}$, followed then by C5 and C3 at 96 and $61 \text{ mg m}^{-2} \text{d}^{-1}$ (Table 4.3).

Table 4.2: Experiment total and cylinder average Volume (ml) and Flux ($\text{mg m}^{-2} \text{d}^{-1}$) data for ebullition events from cylinders 1, 3, 4, and 5.

Cylinder	Ebullition Volume (ml)		CH_4 Flux ($\text{mg m}^{-2} \text{d}^{-1}$)	
	Total	Average	Total	Average
C1	4369	37	33093	384
C3	350	6	1471	61
C4	256	3	1473	122
C5	309	4	1722	95

Cylinders 1, 3, 4 and 5 had a combined total of 391 ebullition events, of those, 71% occurred during periods of decreasing atmospheric pressure (Figure 4.4) (data shown for C1 only, data for C3, C4 and C5 not shown). During the experiment, 339 pressure periods (periods during which atmospheric pressure was consistently increasing or decreasing) were recorded; 170 of increasing pressure, 169 of decreasing pressure. 17% of increasing pressure periods contained ebullition events, and 41% of falling pressure periods contained ebullition events.

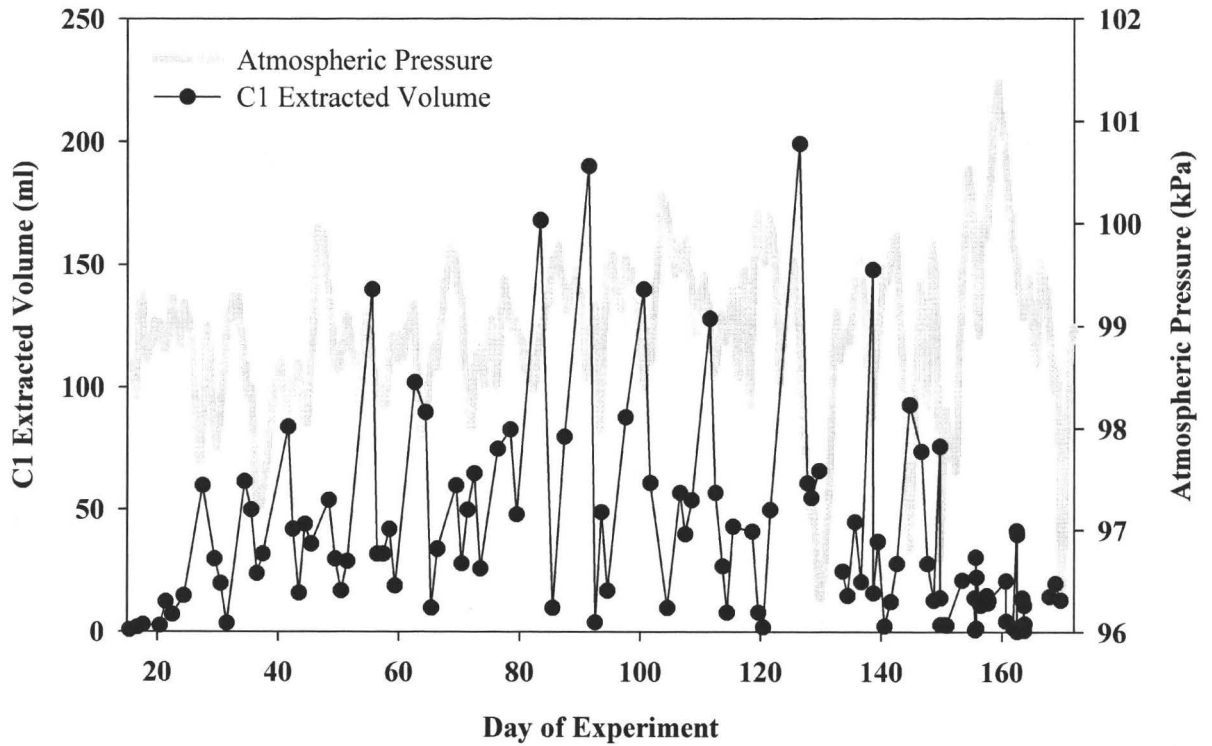


Figure 4.3: Extracted ebullition volume for C1 and atmospheric pressure.

Table 4.3: Ebullition events by cylinder and percent occurrence based on direction of atmospheric pressure change, where % +P Ebullition and % -P Ebullition represent the percent of ebullition occurrences during periods of increasing and decreasing pressure respectively.

Cylinder	Ebullition Events	% +P Ebullition	% - P Ebullition
C1	144	32	68
C3	80	29	71
C4	86	27	73
C5	81	30	70
Combined	391	29	71

Statistical Analysis

Relatively poor linear relationships exist between the dependent (Average Ebullition Flux, Total Ebullition Volume, Average %CH₄ by Volume) and independent (Magnitude, Duration and Rate of each decreasing pressure period) variables examined in this study. Regression analyses however, show some of these relationships to be significant.

Significant relationships exist between Magnitude and Total Volume for cylinders C1, C3 and Combined (Table 4.5). Duration displayed a significant relationship with Total Volume for C1, C3, C4 and the averaged category. No significant relationships exist between Rate as an independent variable and Total Volume of ebullition. C5 showed no significant relationship between Total Volume and any of the independent variables tested.

Table 4.4: P-values for linear regressions between Total Ebullition Volume (dependent variable) and the independent pressure characteristics (Magnitude, Duration and Rate) and combined variable groups, MD (Magnitude & Duration), MR (Magnitude & Rate) DR (Duration and Rate) and MDR (Magnitude, Duration & Rate). Relationships with a 90% confidence interval ($P < 0.100$) are significant and shown shaded.

	Cylinder	Magnitude (kPa)	Duration (Days)	Rate (kPa day ⁻¹)	MD	MR	DR	MDR
Total Volume (ml)	C1	0.015	0.000	0.712	0.002	0.001	0.001	0.003
	C3	0.053	0.021	0.365	0.069	0.097	0.067	0.148
	C4	0.385	0.085	0.877	0.186	0.569	0.233	0.171
	C5	0.211	0.369	0.264	0.465	0.444	0.418	0.635
	Combined	0.000	0.000	0.387	0.000	0.000	0.000	0.000

No consistent relationship was found to exist between the independent variables and Average Flux or Average % CH₄ by Volume (data not shown). C1 and C5 showed a significant relationship between Rate and Average Flux, however C5 does not display relationships common in other cylinders, and therefore this relationship is assumed to be non-indicative of a general relationship (data not shown).

Magnitude and Duration (MD), Magnitude and Rate (MR), and Duration and Rate (DR) variable combinations showed significant relationships to Total Volume for C1, C3 and Combined. The Magnitude, Duration and Rate (MDR) category showed a significant relationship only for C1 and combined.

When paired with Magnitude or Rate, Duration more strongly influenced model predictions for Total Volume values (Table 4.6). Magnitude, when combined with Rate was more influential in predicting Total Volume values. Duration has the greatest effect

on Total Volume when combined with other independent variables and for the greatest number of cylinders when tested independently.

Table 4.5: P-values showing the relative significance of each independent variable (Magnitude, Duration and Rate) in a combination for predicting Total Volume as a dependent variable. This provides insight into the effect of each relative to one another for predicting Total Volume.

Combination		C1	C3	C4	C5	All
Magnitude	M	0.701	0.732	0.723	0.259	0.585
& Duration	D	0.012	0.199	0.597	0.187	0.013
Magnitude	M	0.000	0.052	0.298	0.762	0.000
& Rate	R	0.006	0.325	0.538	0.530	0.026
Duration &	D	0.000	0.033	0.092	0.475	0.000
Rate	R	0.353	0.676	0.928	0.334	0.834
Magnitude,	M	0.631	0.859	0.149	0.946	0.463
Duration	D	0.529	0.389	0.052	0.734	0.222
and Rate	R	0.215	0.769	0.198	0.654	0.591

4.2 Discussion

Entrapped gas variability

Smaller, more temporally frequent fluctuations observed in V_g likely occur in response to production, ebullition and changing environmental conditions, which for the purposes of this experiment are temperature and atmospheric pressure. Although these fluctuations are relatively small, they could have a significant effect on peatland processes including buoyancy, and water and solute transport via changing hydraulic conductivity and gradients.

Numerous studies (e.g. Waine *et al.*, 1985; Reynolds *et al.*, 1992; Beckwith and Baird, 2001) have examined the effect of entrapped gas on hydraulic conductivity in peat, finding that as V_g increases, hydraulic conductivity decreases, and upon elimination of biogenic gas production, hydraulic conductivities begin to increase to levels approaching those immediately after wetting. Beckwith and Baird (2001) found that changes in entrapped gas volume of only 1% could elicit an order of magnitude decrease in hydraulic conductivity within their peat cores, suggesting that the intermediary fluctuations in V_g observed in this study may have a notable influence on peatland function, particularly hydrology.

In a 10-litre volume of peat similar to the cylinders in this experiment, a gas content of 10% is equal to one litre of entrapped gas. To generate an order of magnitude change in hydraulic conductivity, only a 10 ml change in gas volume would be required.

The total range in V_g experienced as a result of these intermediary fluctuations was between 1.2 and 7.0% (Table 4.1), which for some probe locations is similar to or larger than the cumulative change in V_g observed over the experiment. These ranges represent the potential change in V_g possible as a result of intermediary fluctuations. The size of which illustrates the relative potential of intermediary fluctuations to control and influence hydrological processes in peat within the larger patterns in V_g (e.g. seasonal and interannual fluctuations), and therefore to affect other physical and biogeochemical processes in peat.

Maximum individual fluctuations measured during the experiment of increasing V_g were between 0.4 and 4.0%, and decreasing maximums were between 0.7 and 3.0% (Table 4.1), indicating that a single fluctuation could have a major effect. Average intermediary fluctuations in V_g were smaller, approximately 0.2%, however given the magnitude of the effect of a 1% change in entrapped gas, it seems reasonable to hypothesize that even these relatively small fluctuations would have an effect on hydrological processes and peat, and therefore likely on biogeochemical processes associated with them.

Some variation exists between incubation temperatures, and at different probe locations within cylinders (Table 4.1). Direct comparison between incubation temperatures is not possible due to differing incubation lengths, however by comparing C1 and C6 incubated at 20°C and 4°C for the duration of the experiment, there does appear to be an increase in fluctuation magnitude with increasing temperature (Table 4.1

and Figure 4.1). Temporally, fluctuation size and duration were highly variable, occurring over periods of several hours to several days. The combined variability of magnitude and duration both temporally and spatially indicates that peat may have a much more variable hydrological environment than currently thought with fluctuations in processes on relatively small scales within a single site.

Ebullition variability

Given the steady increase in V_g at the 4°C and 11°C incubation temperatures, it seems probable that given enough time, all incubation temperatures would have yielded ebullition events, however given the failure of the climate chamber and the limited incubation time, ebullition only occurred in cylinders incubated at 20°C. As such, analysis of ebullition in this thesis is concerned only with the 20°C incubation temperature.

C1 generated the largest and greatest number of ebullition events. This may in part be attributable to the different incubation periods at 20°C for cylinders 1 and 3, 4 and 5, where C1 was incubated at 20°C for the full 172 days of the experiment, and C3, C4 and C5 were incubated at 20°C for the last 94 days, providing higher production rates for a longer period during the experiment. When increased from 11°C to 20°C, there may have been a lag between increased incubation temperature and adjustment in peat temperatures in C3, C4 and C5, however without internal temperature data, this cannot be determined.

There appears to be a link between bulk density and ebullition characteristics measured during this experiment. Given that bulk density is an indicator of the ability of peat to constrain gas, it follows that there may be a relationship with ebullition. By examining ebullition from the initial onset as events per day to reduce the influence of different 20°C incubation periods, it was found that although C1 had the greatest number of events, C4 had the highest event frequency, followed by C5, C1 and C3. If this is then compared against bulk density information from Chapter 3 (Table 3.1), we find that C4 has the lowest bulk density, followed by C5, C1 and C3 in ascending order. As bulk density increases, pore-size decreases generating stronger capillary forces restraining entrapped gas, further reducing its mobility. As such, without a significant increase in gas production, we could expect a decrease in ebullition event frequency, as a larger volume of gas is required to initiate an ebullition event.

Supporting evidence can be taken from the average volume of ebullition events from C3, C4 and C5; C1 cannot be directly compared to other cylinders due to the longer incubation period at 20°C. If the volume of gas required to initiate an ebullition event increases with increasing bulk density, we might expect the volume of gas released per ebullition event to similarly become larger. C3, having the highest bulk density showed the lowest rate of ebullition occurrence, but also had the largest average volume per event (Table 4.2). Similarly, in descending order of average bulk density, C5 and C4, had decreasing average gas volumes per event and increasing event frequencies.

Similar effects can be seen on a larger scale when considering ebullition from near-surface and deep peats, where deep peats have higher bulk densities than those near the surface (Boelter, 1965) resulting in higher losses by ebullition. Ebullition volumes per day from shallow peat cores were ~ 4.7 to 32.4 ml d^{-1} (Baird *et al.*, 2004; Tokida *et al.*, 2005a; Kellner *et al.*, 2006) with the largest reported event being $\sim 200 \text{ ml}$ (Kellner *et al.*, 2006). Deep peats show less frequent ebullition events (Glaser *et al.*, 2004), but are generally much larger in size as indicated by the sudden changes in surface elevation reported by Glaser *et al.* (2004) of between 8 and 32 cm over short time periods. The potential for a relationship between bulk density and ebullition frequency and volume may be important for the further development of ebullition models and for understanding and predicting ebullition processes in natural peatlands.

Although production rates were not measured, it is reasonable to assume that they would vary between and within cylinders based on carbon quality and supply (Baird *et al.*, 2004) and the movement and availability of other substrates required for gas production. This in turn is affected by entrapped gas processes such as changes in hydraulic conductivity and hydraulic gradients as discussed earlier in this chapter. As production rates vary within a cylinder, hotspots for gas production may be generated while other areas may have relatively little activity, affecting gas availability within the cylinder, and therefore ebullition.

A relationship also seems to exist between bulk density and CH_4 concentration in ebullition gases, where lower bulk density peat generates higher CH_4 fluxes from

ebullition (Table 4.2). Given that lower bulk densities are associated with larger pores and increased flow rates, this relationship could be related to increased nutrient availability or a greater supply of labile carbon for methanogenesis, similar to the relationship between proximity to the water table and increases in anaerobic biological activity and CH₄ production (Brown *et al.*, 1989; Sundh *et al.*, 1992).

The ebullition-pressure relationship

Although periods of falling atmospheric pressure accentuate the potential for ebullition, they do not always elicit this response (Glaser *et al.*, 2004; Strack *et al.*, 2005). The irregular response of ebullition to periods of falling pressure has been noted in this study, demonstrating that there are other considerations to be made when examining the relationship between decreasing atmospheric pressure and ebullition. As noted by Fechner-Levy and Hemond (1996) and later by Baird *et al.* (2004), some critical volume of gas, must be exceeded for ebullition to occur so that a decrease in pressure will only initiate ebullition if it causes V_g to exceed this value. Following an ebullition event, V_g will build-up during which, periods of falling atmospheric pressure, although they increase gas volume according to the Ideal gas law and Henry's law (Fechner-Levy and Hemond, 1996; Tokida *et al.*, 2005; Kellner *et al.*, 2006), may not be sufficient to instigate an ebullition event. The result being that periods of falling atmospheric pressure do not in themselves cause ebullition, but can help existing entrapped gas to overcome the forces restraining it.

Within the relationship between declining atmospheric pressure and ebullition, different characteristics of falling pressure have the potential to influence ebullition differently because of other processes involved in entrapped biogenic gas dynamics including production, internal gas movement and bubble coalescence. Results from this study indicate the duration and the magnitude of a period of falling pressure have varying degrees of influence on the size of ebullition events that occur. Duration appears to have a larger effect on event volume (3 of 4 cylinders) compared to the magnitude of the event, which showed a relationship in two of the four cylinders, and the relationships are consistently stronger for duration than for magnitude.

Assuming that gases compensate instantaneously for environmental changes (temperature and atmospheric pressure), we can compare the effects of both magnitude and duration in affecting ebullition event volume. A drop in atmospheric pressure of short duration (e.g. 12 hours) and large magnitude (e.g. 1.5 kPa) will cause entrapped gas to expand (Ideal gas law) (Fechner-Levy and Hemond, 1996), and will release a volume of gas approximately equal to the induced volume increase (Tokida *et al.*, 2005a) should it exceed the restraining forces of the peat based on this increase in volume (Baird *et al.*, 2004). A decrease in pressure of the same magnitude (kPa) over a longer duration (e.g. 2 days) may provide time for buoyant forces of deeper bubbles to overcome local restraining capillary forces moving them through the peat column, allowing them to coalesce with other bubbles, increasing their cumulative buoyant force, where during a short drop they may have been 're-trapped' in the peat matrix. Coalescing bubbles will increase their cumulative buoyant force more gradually at a location with higher

structural strength or narrower pore-pathways (stronger capillary forces), accumulating to a volume sufficient to overcome these restraining forces and escaping. Without this coalescing, they may not reach a common new obstacle, remaining dispersed through the cylinder, with smaller buoyant forces working against the restraining forces of the peat.

No significant relationship appears to exist between CH₄ flux or percent CH₄ by volume and either characteristic of pressure decreases. These ebullition characteristics are based on production rates, and nutrient and substrate availability, which are not notably affected by variations in atmospheric pressure (Knowles, 1993; Segers, 1998).

Implications

Changes in V_g , both small and large scale, occur in response to changes in external conditions that impose themselves on peatland systems. At the large scale these may consist of interannual variability in overall climate (e.g. warm and dry vs. cool and wet) and also intra-annual changes between seasons. These large changes may generate fluctuation in V_g on the order of 10's of percents, resulting in significant variability in hydrologic conditions, which in turn will potentially influence all other peatland processes, including feedbacks to entrapped gas processes. At the smaller scale, V_g variability on the order of 1-5% may be generated by fluctuations in pressure and smaller temperature changes, by variations in gas production and ebullition creating further patterns. Both the large and small fluctuations in V_g allow peatland systems to maintain themselves within a range of conditions favourable to their productivity and persistence.

Ebullition frequency in natural peatlands will increase with increasing temperature because of the effect of temperature on internal gas dynamics resulting in increased event size and therefore, total CH₄ flux to the atmosphere (Fechner-Levy and Hemond, 1996; Strack *et al.*, 2005). If we consider a warm year and a cool year with equal precipitation, the warmer year would have higher gas production and ebullition events, with resultant increases in CH₄ flux to the atmosphere compared to a cool year. As such, during warm years peatlands may act as more significant sources of CH₄ to the atmosphere than cooler years. With the potential for increasing temperatures with climate change then, we could expect to see peatlands as an increased source for CH₄ (Strack *et al.*, 2005).

Entrapped gas as a coupled ecohydrological feedback mechanism

Inter-annual fluctuations in climate and non-natural climate change have a direct effect on CH₄ production and therefore its release to the atmosphere (Strack *et al.*, 2005). In colder climates, even a relatively small change in temperature could generate large changes in gas dynamics and release from peatlands when compounded over all affected peatlands with active gas processes.

Fluctuations in climate also impact moisture conditions within peatlands, and therefore microform and peatland development. The processes of moisture availability and microform development discussed by Belyea and Clymo (2001) appear also to be very closely linked to gas dynamics in peatlands. Vegetation responds to changing environmental conditions affecting gas production and gas storage, which in turn affect

moisture conditions which feeds back into vegetation cover and microform development based on moisture conditions as discussed by Belyea and Clymo (2001). The resultant variability in bulk density reflects the spatial (areal and depth) distribution of gas stores within and across a peatland (Tokida *et al.*, 2005b). Gas bubbles and therefore their distribution, affects diffusion gradients (Rothfuss and Conrad, 1998) and ebullition occurrence (Baird *et al.*, 2004) so that the high degree of variability in gas storage can in part explain the high degree of variability in both diffusive and ebullition fluxes seen in peatlands (e.g. Moore and Knowles, 1990; Walter *et al.*, 1996; Strack *et al.*, 2005). Consequently, entrapped gas can be viewed as a coupled feedback to peatland ecohydrology, highlighting the importance of entrapped gas variability in field investigations of peatland hydrology.

CHAPTER 5: MODELING ENTRAPPED GAS CONTENT

5.1 Results

Modeled entrapped gas content

Gas production values, representing total gas added (ml) to the system and CH₄ production values (ug m⁻¹ d⁻¹), are highest at ~20°C incubation temperatures, and decrease with decreasing temperature (Table 5.1).

Table 5.1: Production values (ml d⁻¹) used in the model. CH₄ production values (ug g⁻¹ d⁻¹) were based on average ebullition CH₄ concentration per cylinder. The number of days over which each production value was applied are also presented. Values are in order of use from the beginning to the end of the model dataset (days 210-330, 120 days).

Cylinder		Gas (ml day ⁻¹)				CH ₄ (ug g ⁻¹ d ⁻¹)				Duration (Days)			
		Production				Production							
C1	L	32	40	30		16	20	15		44	19	57	
	U	40	37	30		20	19	15		29	34	54	
C3	L	1	3.5	6	20	0.2	0.8	1	5	30	33	15	42
	U	1	10	1		0.2	2	0.2		29	33	58	
C4	L	1	0.5	6		0.4	0.2	2		26	15	79	
	U	1	4			0.4	1			30	90		
C5	L	1	5			0.4	2			44	76		
	U	1	0.5	5		0.4	0.2	2		30	44	76	
C6	L	0.5				n/a*				120			
	U	0.5				n/a*				120			

* Bulk density values were not available for CH₄ production estimation

Production in C1 showed an initial increase followed by a decline towards the end of the experiment. The change in incubation temperature for C3, C4 and C5 from ~11°C to ~20°C on day 78 of the experiment generated an increase in gas production with the exception of C4L, which had a period without any notable gas accumulation. C6, stored

at $\sim 4^{\circ}\text{C}$, had the lowest gas production rate (0.5 ml d^{-1}) maintained for the duration of the experiment.

Model results based on pressure and temperature show patterns that correspond with the measured ΔV_g values, however, with the exception of C1U, the addition of gas production and ebullition improved model fit (Table 5.2). Generally, model results agreed with measured ΔV_g values most closely from the beginning to the middle of the period investigated. Towards the end of the model run, there was a general separation from measured values where the model tended to slightly over-estimate entrapped gas volumes. This trend was less pronounced in C3, and most evident in C4 and C5. Ebullition was most active in C1 and the inconsistent nature of these events is evident in the relationship between measured and calculated ΔV_g values (Figure 5.1 and Figure 5.2).

Table 5.2: r^2 values based on measured ΔV_g values and ΔV_g as calculated by the model accounting for atmospheric pressure and temperature changes only (P&T) and where pressure, temperature, production and ebullition were included (P, T, Prod & Eb.).

Cylinder	Model r^2 Values	
	P & T	P, T, Prod & Eb
C1	Lower	0.00
	Upper	0.74
C3	Lower	0.47
	Upper	0.59
C4	Lower	0.56
	Upper	0.57
C5	Lower	0.54
	Upper	0.39
C6	Lower	0.00
	Upper	0.20

* In the case of C2, no ebullition data was available, and therefore is not presented here.

The ability of the model to estimate changes in entrapped gas content varies between cylinders and probe location (Table 5.2). Cylinder 3 yielded the best fit between calculated and measured ΔV_g values although some outliers were not accounted for by the model (Figure 5.2), followed by C5, C4, C1 and C6 in order of descending goodness of fit.

Within the cylinders, individual probe locations had varying degrees of fit and the model was unable to reasonably predict changes in entrapped gas volumes for C4U, C5L and for both C6L and C6U. Entrapped gas contents (V_g) at these probe locations were below 0.1, and the model consistently over-predicted the level of variability compared to that seen in the measured ΔV_g . After warming to 20°C, and the resultant increase in gas content, model results for C4U and C5L improved. In the case of C6, the values calculated by the model were an order of magnitude different from measured values for the duration of the model period.

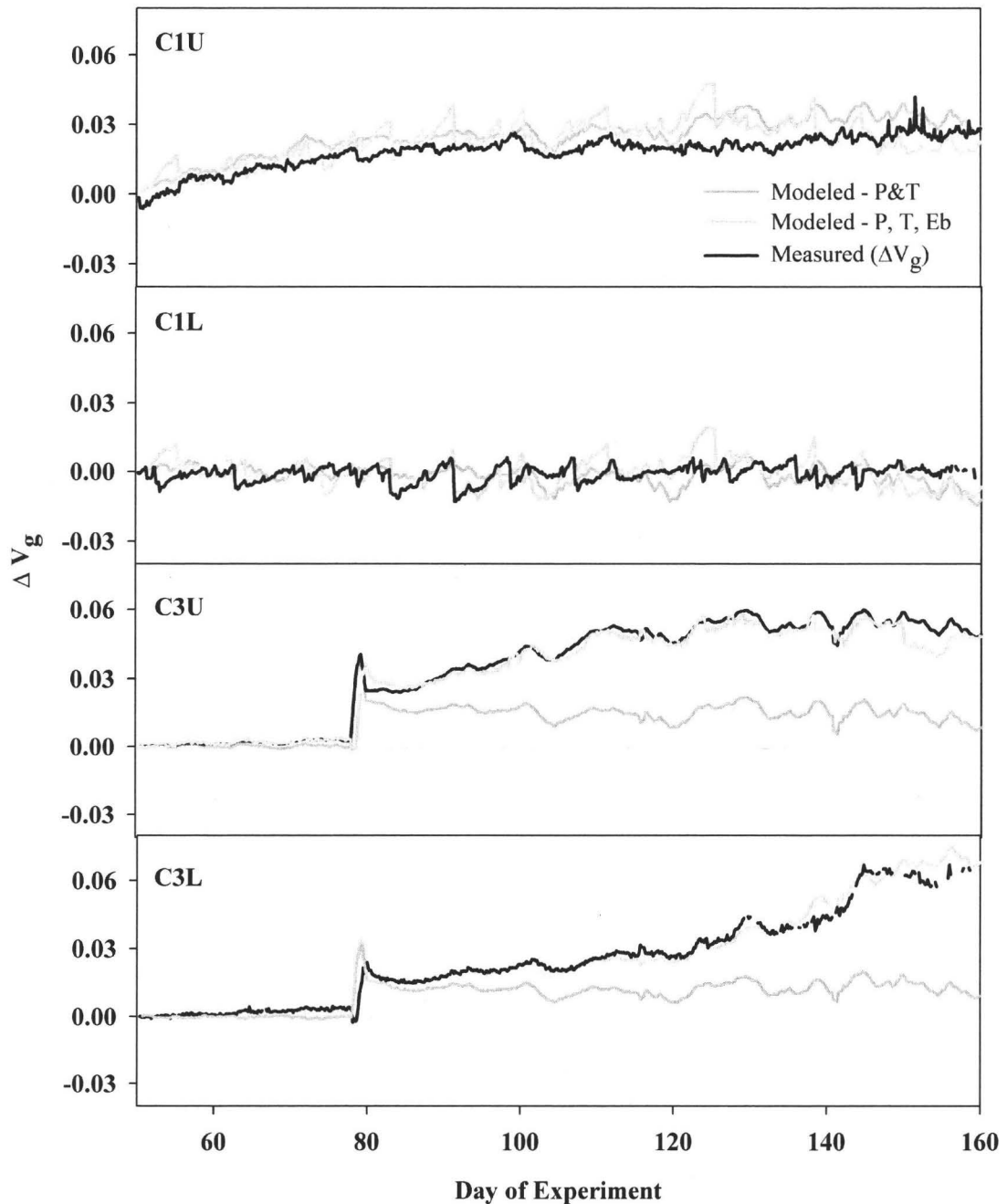


Figure 5.1: Measured and calculated ΔV_g values for C1 and C3. The black line indicates measured ΔV_g , calculated ΔV_g values for the P, T, Prod. & Eb and the P & T models are indicated by the light grey and dark grey lines respectively.

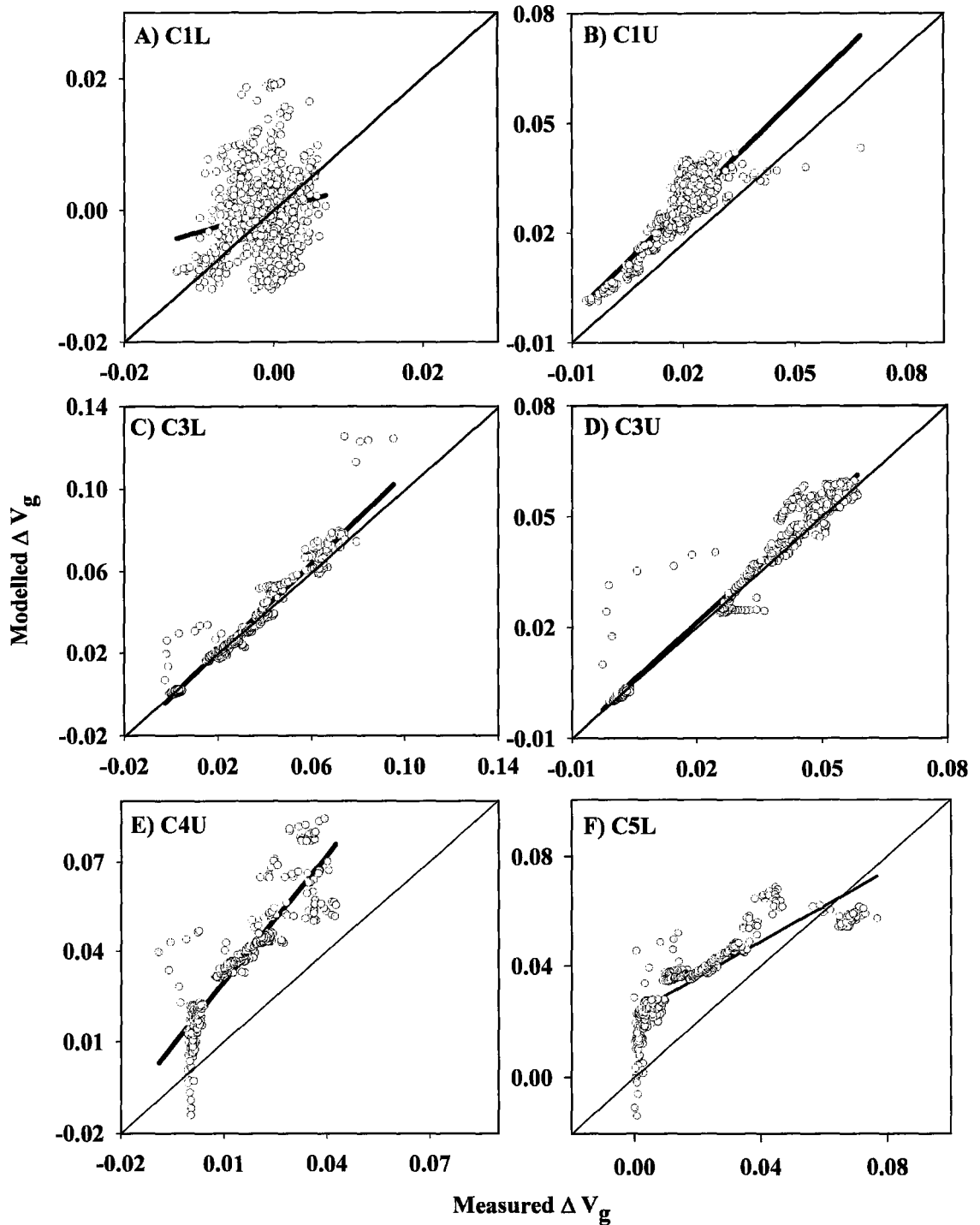


Figure 5.2: Scatter plots of measured ΔV_g values against calculated values for the model that best fits the measured data. Measured C1U values are plotted against the P&T model, the remainder of the cylinder locations are plotted against calculated values from the P, T, Prod. & Eb model. Regression lines and 1:1 lines are also plotted.

5.2 Discussion

Modeled entrapped gas content

Results from the model demonstrate that intermediary fluctuations in V_g are largely attributable to changes in atmospheric pressure and small fluctuations in temperature, however production and losses via ebullition also impact patterns in V_g . The ability of the model to reasonably predict the spike in gas content displayed in C3, C4 and C5 when the climate chamber failed and over-heated on day 78 also seems to indicate that temperature is a major component of volume increases in entrapped gas over large temperature regime changes, however the relative importance of changing production was not evaluated in this work.

Although general trends in V_g show a good fit between modeled and measured values, the treatment of production and ebullition, and conditions where V_g is $<10\%$ need to be further addressed. By increasing the timescale over which ebullition is measured and improving methods of estimating production, model results could be improved. There is potential for a compounding effect due to the offset between ebullition measurements and TDR-measured V_g , where over a 24-hour period, a TDR probe may measure numerous events of smaller magnitude; a single ebullition event of large magnitude may be recorded from the gas trap, affecting how it is represented in the model. Moreover, measuring V_g at more depths or by employing other geophysical techniques (e.g. Comas *et al.*, 2005) to gather further information about internal gas distribution may improve our understanding of entrapped gas processes.

The use of a linear relationship between changes in atmospheric pressure, temperature and changes in EAPCs do not appear to accurately represent the conditions where entrapped gas contents are <10%, and further work should investigate means by which the relationship can be better represented in these scenarios. As a first approximation however, this model successfully illustrates the importance of temperature and atmospheric pressure in generating fluctuations in entrapped gas within peat.

CHAPTER 6: CONCLUSIONS

This research has shown consistent undersaturation of near surface peat under laboratory conditions, supporting similar findings by Baird *et al.*, (2004). The persistence of a gas phase within the cylinders and potential air entrapment during wetting events (infiltration and water table rise), in natural peatlands would allow Henry's law and the Ideal gas law to control the partitioning of gases between the aqueous and gaseous states as it is produced. As such, while initial bubble formation by nucleation above EAPCs may be an important mechanism deeper in the peat profile, it is not likely the dominant process in near-surface peat. Current peatland models that allow for initial bubble formation only after surpassing EAPC values may not accurately represent CH₄ processes in near-surface peats, and would not account for the potential variability in processes with depth.

The control of Henry's law and the Ideal gas law are such that V_g fluctuates in response to changes in atmospheric pressure and temperature. These fluctuations occur on various temporal scales with the potential for large fluctuations associated with inter-annual climatic variability (e.g. warm and dry vs. cool and wet) and also intra-annual seasonal variations. Changes in entrapped gas content have been shown to have a significant effect on hydrological conditions (e.g. Reynolds *et al.*, 1992), which in turn may influence other peatland processes, including feedbacks to entrapped gas processes. While some effects of changes in V_g have been well documented, smaller, more frequent

fluctuations in V_g in response to relatively small temperature fluctuations and changes in atmospheric pressure have not previously been investigated. This research has shown that variations in V_g of up to 4 % may be generated on a scale of hours by variations in temperature, atmospheric pressure, gas production and ebullition. Based on current literature, some measured fluctuations were large enough to significantly influence hydrological conditions, and there is potential for the smaller average fluctuations to generate a measurable response as well.

To investigate the influence of temperature and atmospheric pressure on generating these fluctuations, a model was used to estimate changes in entrapped gas (ΔV_g) using measured values from the experiment. General trends in ΔV_g showed a good fit between modeled and measured values, however the treatment of production and ebullition where V_g is <10% need to be further addressed. This work illustrates that although the basic intermediary changes in V_g can be predominantly attributed to changes in environmental (pressure and temperature) conditions, at the small scale there is a departure between measured and modeled ΔV_g , indicating that there are other factors involved that have not yet been accounted for. As a first approximation however, this model successfully illustrates the importance of temperature and atmospheric pressure in generating fluctuations in entrapped gas within peat and could in future have applications in peatland hydrological modeling.

There appears to be a relationship between bulk density and biogenic gas processes in peat. As bulk density increases, the frequency of ebullition occurrence

(events d^{-1}) decreases, while the average size of each event increases. As bulk density increases, pore-size decreases therefore strengthening capillary forces, reducing gas mobility. As such, the buoyant forces, and therefore the volume, of gas must be greater to move through the peat. Therefore, the frequency of ebullition events will decrease, but the volume of gas released will on average increase with increasing bulk density. Evidence of these effects was shown in the differences between C3, C4 and C5 ebullition measured during their 20°C incubation period. Some relationship may also exist between bulk density and gas production related to the transport and availability of solutes and substrates for gas production and carbon quality. The potential for a relationship between bulk density and ebullition frequency and volume may be important for the further development of ebullition models and for understanding and predicting ebullition processes in natural peatlands. However, further investigation of the influence of bulk density is required before further characterization of this relationship can be done.

Falling atmosphere pressure has been linked to the occurrence of ebullition events due to its effect on gas volume. As pressure decreases, V_g volume increases according to the Ideal gas law, potentially providing the increase in buoyant force required to exceed restraining forces of the peat. Indeed, results from this research found that although ebullition occurs at other times, 71 % of ebullition events occurred during periods of decreasing pressure indicating that there is a strong relationship between these events. The duration of falling pressure periods had a greater effect on ebullition volume than the magnitude of the pressure drop, although both have strong relationships. Given this, for an equally large pressure drop that occurs over a short vs. long period of time, the drop of

longer duration although no bigger will cause a larger volume to be released. This may be related to the coalescence of bubbles within the peat over longer periods of time allowing them to aggregate their buoyant forces, allowing an increased volume of gas to exceed the threshold of the peat. Differentiating between the effects of different characteristics of falling pressure on ebullition adds to our understanding of the ebullition-pressure relationship. A better understanding of how pressure interacts with entrapped gas processes and gas thresholds will also assist in developing more accurate models which will help develop our understanding of peatlands as a source of CH₄ to the atmosphere and their role in the global carbon cycle.

REFERENCES

- Baird, A.J., Waldron, S. (2003) Shallow horizontal groundwater flow in peatlands is reduced by bacteriogenic gas production. *Geophysical Research Letters* 30(20) doi: 10.1029/2003GL018233.
- Baird, A.J., Beckwith, C.W., Waldron, S., Waddington, J.M. (2004) Ebullition of methane-containing gas bubbles from near-surface *Sphagnum* peat. *Geophysical Research Letters* 31, L21505, doi: 10-1029/2004GL01\21157.
- Beckwith, C.W., Baird, A.J. (2001) Effect of biogenic gas bubbles on water flow through poorly decomposed blanket peat. *Water Resources Research* 37(3): 551-558.
- Belyea, L.R., and Clymo, R.S. (2001) Feedback control of the rate of peat formation. *Proceedings of the royal society of London series B – Biological Sciences* 268 (1473): 1315-1321.
- Boelter, D.H. (1965). Hydraulic conductivity of peats. *Soil Science*, 100: 227-231.
- Brown, A., Mathur, S.P., Kushner, D.J. (1989) An ombrotrophic bog as a methane reservoir, *Global Biogeochemical Cycles*, 3: 205-213.
- Buttler, A.J., Dinel, H., Levesque, M., Mathur, S.P. (1991) The relation between movement of subsurface water and gaseous methane in a basic bog with a novel instrument, *Canadian Journal of Soil Science*, 71: 427-438.
- Clymo, R.S. (1983) Peat. In: Gore, A.J.P. (Ed.), *Mires: Swamp, Bog, Fen and Moor*, Elsevier Scientific, New York, pp. 159-224.
- Clymo, R.S. (1984) The limits to peat bog growth. *Philosophical transactions of the London royal society series B – Biological Sciences* 303(1117): 605-654.
- Constantz, J., Herkelrath, W.N., Murphy, F. (1988) Air encapsulation during infiltration, *Soil Science Society of America Journal*, 52: 10-16.
- Dean, J.A. (1999) Lange's Handbook of Chemistry, 15th Edition. *Toronto: McGraw-Hill Inc.*
- Devito, K.J., Waddington, J.M., Branfireun, B.A. (1997) Flow reversals in peatlands influenced by local groundwater systems. *Hydrological Processes* 11: 103-110.
- Dinel, H., Mathur, S.P., Brown, A., Levesque, A. (1988) A field study of the effect of depth on methane production in peatland waters: Equipment and preliminary results. *Journal of Ecology* 76: 1083-1091.

- Dunfield, F., Knowles, R., Dumont, R., Moore, R. (1993) Methane production and consumption in temperate and subarctic peat soils: response to temperature and pH. *Soil Biology Biogeochemistry* 25(3): 321-326.
- Environment Canada (2004) Hourly weather data, Climate normals and averages www.climate.weatheroffice.ec.gc.ca.
- Faybishenko, B.A. (1995) Hydraulic behavior of quasi-saturated soils in the presence of entrapped air: Laboratory experiments, *Water Resources Research* 31: 2421-2435.
- Fayer, M.J., Hillel, D. (1986) Air encapsulation, 1, Measurement in a field soil, *Soil Science of America Journal*, 50: 568-572.
- Fechner-Levy E.J., Hemond, H.F. (1996) Trapped methane volume and potential effects on methane ebullition in a northern peatland. *Limnology and Oceanography* 41(7): 1375-1383.
- Frenkel, J. (1955) Kinetics of phase transfers, in *Kinetic Theory of Liquids*, pp 366-413, Dover, New York.
- Girard, M. (1999). The natural revegetation of highly disturbed wetlands: mined peatlands of Southern Québec MSc Thesis, Département de Géographie, Université Laval, Sainte-Foy, Québec, Canada.
- Glaser, P.H., Chanton, J.P., Morin, P., Rosenberry, D.O., Siegel, D.I., Ruud, O., Chasar, L.I., Reeve, A.S. (2004) Surface deformations as indicators of deep ebullition fluxes in a large northern peatland. *Global Biogeochemical Cycles* 18, GB1003, doi: 10.1029/2006GB002069.
- Gorham, E. (1991) Northern peatlands: role in the carbon cycle and probable response to climatic warming. *Ecological Applications* 1: 182-195.
- Granberg, G., Ottosson-Lofvenius, M., Grip, H., *et al.* (2001) Effect of climatic variability from 1980-1997 on simulated methane emissions from a boreal mixed mire in northern Sweden. *Global Biogeochemical Cycles* 15(4): 977-991.
- Hutchinson, G.E. (1957) A Treatise on Limnology, vol.1 *Geography Physics and Chemistry*, 1015 pp. John Wiley, Hoboken, N.J.
- Ingram, H.A.P. (1983) Hydrology. In: *Ecosystems of the World*, Volume 4A, *Mires: Swamp, Bog, Fen and Moor, General Studies*, Gore AJP (ed). Elsevier: New York; 67-158.

- Ingram, H.A.P. (1992) Introduction to the ecohydrology of mires in the context of cultural perturbation. *In: Peatland Ecosystem and Man: An Impact Assessment*, Bragg, O.M. Hulme, P.D., Ingram, H.A.P. (Tr.) Academic Press, London, p. 276.
- Ivanov, K.E. (1981) *Water movement in mirelands*, translated from Russian by A. Thompson and H.A.P. Ingram, Academic, San Diego, Calif., 1981.
- Johnson, B.D., Boudreau, B.P, Gardiner, B.S., and Maass, R. (2002) Mechanical response of sediments to bubble growth, *Marine Geology* 187: 347-363.
- Kellner E., and Lundin, L.C. (2001) Calibration of time domain reflectometry for water content in peat soil. *Nordic Hydrology* 32(4/5): 315-332.
- Kellner, E., Price, J.P., Waddington, J.M (2004) Pressure variations in peat as a result of gas bubble dynamics. *Hydrological Processes* 18: 2599-2605.
- Kellner, E., Waddington, J.M., Price, J.S. (2005) Dynamics of biogenic gas bubbles in - peat: Potential effects on water storage and peat deformation. *Water Resources Research* 41: W08417, doi: 10.1029/2004WR003732.
- Kellner, E., A. J. Baird, M. Oosterwoud, K. Harrison, and J. M. Waddington (2006), Effect of temperature and atmospheric pressure on methane (CH₄) ebullition from near-surface peats, *Geophysical Research Letters*, 33, L18405, doi:10.1029/2006GL027509.
- Knowles, R. (1993) Methane: Processes of Production and Consumption. *Agricultural Ecosystem Effects on Trace gases and Global Climate Change*. American Society of Agronomy Special Publication no. 55: 145-156.
- Lavoie, C. and Rochefort, L. (1996). The natural revegetation of a harvested peatland in southern Québec:a spatial and dendroecological analysis. *Écoscience* 3: 101-111.
- Mallik, A.U. (1989) Small-scale succession towards fen on floating mat of a *Typha* marsh in Atlantic Canada, *Canadian Journal of Botany* 67: 1309-1316.
- Mitsch, W.J, and Gosselink, J.G. (2000) *Wetlands New York : Van Nostrand Reinhold*.
- Moore, T.R. and Knowles, R. (1990) Methane emissions from fen, bog and swamp peatlands in Québec. *Biogeochemistry* 11: 45-61.
- NWWG – National Wetlands Working Group (2004) Wetland distribution – Wetland regions. <http://wetlands.cfl.scf.rncan.ec.gc.ca>.
- Price, J.S. (1996) Hydrology and microclimate of a partly restored cutover bog, Quebec. *Hydrological Processes*, 1263-1272.

- Price, J.S. (2003) Role and character of seasonal peat soil deformation on the hydrology of undisturbed and cutover peatlands. *Water Resources Research*, Vol. 39, No. 9, 1241.
- Reynolds, W.D., Brown, D.A., Mathus, S.P., Overend, R.P. (1992) Effect of in-situ gas accumulation on the hydraulic conductivity of peat, *Soil Science* 153: 397-408.
- Romanowicz, E.A., Siegel, D.I., Chanton, J.P., Glaser, P.H. (1995) Temporal variations in dissolved methane deep in the Lake Agassiz Peatlands, Minnesota. *Global Biogeochemical Cycles* 9(2): 197-212.
- Rosenberry, D.O, Glaser, P.H., Siegel, D.I., Weeks, E.P. (2003) Use of hydraulic head to estimate volumetric gas content and ebullition flux in northern peatlands, *Water Resources Research* 39: 1066, doi: 10.1029/2002WR001377.
- Rothfuss F., and Conrad, R. (1998) Effect of gas bubbles on the diffusive flux of methane in anoxic paddy soil. *Limnology and Oceanography* 43(7):1511-1518.
- Roulet, NT. (1991) Surface level and water-table fluctuations in a sub-arctic fen. *Arctic and Alpine Research*, 23 (3); 303-310.
- Segers, R. (1998) Methane Production and Methane Consumption: A Review of Processes Underlying Wetland Methane Fluxes. *Biogeochemistry* 41(1): 23-51.
- Slabaugh, W.H., Parsons, T.D. (1976) Solutions, in *General Chemistry*, 3rd ed., chap 12, pp. 203-336, John Wiley, Hoboken, N.J.
- Strack, M., Kellner, E., Waddington, J.M. (2005) Dynamics of biogenic gas bubbles in peat and their effects on peatland biogeochemistry. *Global Biogeochemical Cycles* 19, GB1003, doi: 10.1029/2004GC002330.
- Strack, M. (2006) Ecohydrological controls on peatland carbon cycling following water table draw down. PhD Thesis. McMaster University, Hamilton, Ontario, Canada. 180 Pages.
- Strack, M., Kellner, E., and Waddington, J.M. (2006) Effect of entrapped gas on peatland surface level fluctuations, *Hydrological Processes* 20(17): 3611-3622.
- Sundh, I., Nilsson, M., Svensson, B.H. (1992) Depth distribution of methane production and oxidation in a *Sphagnum* peat bog. *Suo* 5: 367-269.
- Tokida, T., Miyazaki, T., Mizoguchi, M., Seki, K. (2005a) *In Situ* accumulation of methane bubbles in a natural wetland soil. *European Journal of Soil Science* 56: 389-395.

- Tokida, T., Miyazaki, T., Mizoguchi, M. (2005b) Ebullition of methane from peat with falling atmospheric pressure. *Geophysical Research Letters* 32, L13823, doi: 10-1029/2005GL022949.
- Varian (2003). Varian Product Specifications. www.varianinc.com.
- Waddington, J.M. and Roulet, N.T. (2000) Carbon balance of a boreal patterned peatland. *Global Change Biology*, 6: 87-98.
- Waddington J.M., and Roulet, N.T. (1996) Atmosphere-wetland carbon exchanges: Scale dependency of CO₂ and CH₄ exchange on the developmental topography of a peatland. *Global Biogeochemical Cycles*, 10(2): 233-245.
- Waine, J., Brown, J.M.B., Ingram, H.A.P. (1985) Non-Darcian transmission of water in certain humified peats, *Journal of Hydrology* 82: 327-339.
- Walter, B.P., Heimann, M., Shannon, R.D., White, J.R. (1996) A process-based model to derive methane emissions from natural wetlands. *Geophysical Research Letters* 23(25): 3731-3734.
- Walter, B.P., Heimann, M. (2000) A process-based, climate-sensitive model to derive methane emissions from natural wetlands: Application to five wetland sites, sensitivity to model parameters, and climate, *Global Biogeochemical Cycles* 14: 745-765.
- Walter, K.M., Zimov, S.A., Chanton, J.P., Verbyla, D., Chapin, F.S. (2006) Methane bubbling from Siberian thaw lakes as positive feedback to climate warming. *Nature Letters*. 443. doi:10.1038/nature05040.
- Whalen, S.C., Reeburgh, W.S. (1990) Consumption of atmospheric methane by tundra soils, *Nature*, 346: 160-162.